206

EVALUATION OF A FINITE-ELEMENT METHOD TO ANALYZE STEEL AND CONCRETE STRUCTURAL MEMBERS

by

DAVID DAHWEI LEE

B.S., Taiwan Provincial College of Marine and Oceanic Technology, 1974

A MASTER'S THESIS

submitted in partial fulfillment of the

requirements for the degree

MASTER OF SCIENCE

Department of Civil Engineering

KANSAS STATE UNIVERSITY
Manhattan, Kansas

1978

Approved by:

Stuart E Swartz
Major Professor

TABLE OF CONTENTS

TABLE OF CONTENTS (cont'd.)

CHAPTER I

INTRODUCTION

In the past years, composite steel-concrete floor systems have been used in construction practice. The composite construction is economical in buildings for longer spans and large live load intensities. The elastic behavior and load-carrying capacity of composite steel-concrete beams have been well understood.

In the design of multi-story buildings, the economic principles are important as well as the safety factors. When all other factors are approximately equal, the design which results in the lowest structure cost will be considered as the most economical and desirable design. One method of achieving economy in high-rise steel frame buildings is to reduce the building height by introducing web openings in the floor beams to permit the passage of utility ducts and pipes. Thus, the space from the floor of one story to the ceiling of the story below will be reduced, so that the overall building height will be lowered. Many research programs on the effect of web openings on the behavior of non-composite steel beams have been conducted. But neither the composite steel-concrete theory nor the theories of non-composite steel beams with web openings can be applied directly to composite steel-concrete beams with web openings.

The primary objective of this thesis was to determine the suitability of a finite element program which was developed by

Michael Taylor (14) at the University of California at Davis for problems associated with composite beams with web openings. In this study, the program was used to model non-composite steel beams, reinforced concrete beams, composite steel-concrete beams without web openings and composite beams with web openings. Three types of elements are combined in this program: plane stress (or strain) continuums, reinforcing bending elements ("beams") and bond elements. Numerical results obtained from the finite element computer program analysis were compared with those obtained from other methods of analysis.

CHAPTER II

LITERATURE REVIEW

2.1 Non-Composite Steel Beams With Web Openings

Research concerning the elastic behavior of non-composite steel beams with openings in their webs has been conducted by many groups and organizations. In 1958, Heller, Brock and Bart presented a solution by the complex variable method associated with Muskhelishvili for the stresses around a rectangular opening in a uniformly loaded plate (1). In 1962, they again presented a paper in which the stresses around a rectangular opening in a beam subjected to bending and shear were investigated (2).

In 1966, Bower developed an analytical method for calculating stresses around elliptical holes in a wide-flange beam under a uniform load (3). In the same year, he conducted tests on simply supported wide-flange beams with circular or rectangular web openings loaded by concentrated loads (4). He concluded that for circular and rectangular holes the elastic analysis could accurately predict the tangential stress along the hole and the bending stress on transverse cross sections in the vicinity of the hole when the hole did not exceed half of the web depth. In his studies, Vierendeel Analysis was used to predict a reasonably accurate bending stress except for local stress concentrations at the hole corners.

Ultimate strength analyses and tests have also been reported in recent years. In 1968, Bower presented a paper concerned with Ultimate Strength of Beams with Rectangular Holes (5). In the same year, Redwood and McCutcheon conducted the beam tests with unreinforced web openings (6). In 1972, Cooper and Snell performed tests on beams with reinforced web openings and confirmed the validity of Vierendeel Analysis for the estimation of the normal stresses in the vicinity of the hole (7).

2.2 Composite Steel-Concrete Beams Without Web Openings

Composite steel-concrete beam studies in the United States were started in 1929 (8). During the period 1929-1958, investigations of composite beams without web openings were carried out both experimentally and theoretically. Before the 1950's, composite construction was primarily utilized in highway bridges. In 1960, Viest (9) reviewed and listed the references describing the composite beam tests. He also reviewed the studies of elastic theories and ultimate strength theories of the composite beams (9).

A State-of-Art report on composite construction published in 1974 listed recently conducted research in this country (10).

2.3 Composite Steel Beams With Web Openings

The results of the investigations for non-composite beams with web openings and composite steel beams without

web openings cannot be directly applied to the composite steel beams with web openings.

In 1964 and 1966, Larnach and Giriyappa tested some castellated composite T-Beams (11,12), but the web openings in castellated beams have different shapes than those normally used in W-shape beams. Therefore, the results of this research probably cannot be applied to the present problem.

In 1968, Granade reported the results of elastic and ultimate load tests on two composite beams with rectangular web openings (13). The data obtained from his research was not sufficient to accurately determine the distribution of the shear forces around the openings. He also concluded that the failure in both ultimate load tests was by diagonal cracking in the concrete slab.

CHAPTER III

TAYLOR'S COMPUTER PROGRAM

3.1 Material Property Assumptions

3.1.1 Steel

The typical stress-strain curves for both normal steel and prestressing steel shown in Fig. 3.1 are used for this program. The Poisson's ratio for all steel used as reinforcing ("beam") elements is assumed to be constant throughout all possible ranges of loading. Although this assumption is incorrect in the plastic range, there is no significant error when using this type of element. The uniaxial modulus values are assumed to be based upon the axial stress condition in the steel.

If steel is used as a continuum material, the plastic properties are based on any reasonable biaxial failure criterion.

3.1.2 Concrete

Concrete has a uniaxial compressive strength between 2000 and 8000 psi and uniaxial tension strength of about one-tenth the compressive strength (14). Plain concrete is essentially linear and elastic in tension but is nonlinear when subjected to compressions greater than about one quarter of its uniaxial strength (Fig. 3.2). If unloading occurs, as shown at points P and Q, it has been observed that the concrete unloads along lines parallel to the initial tangent modulus.

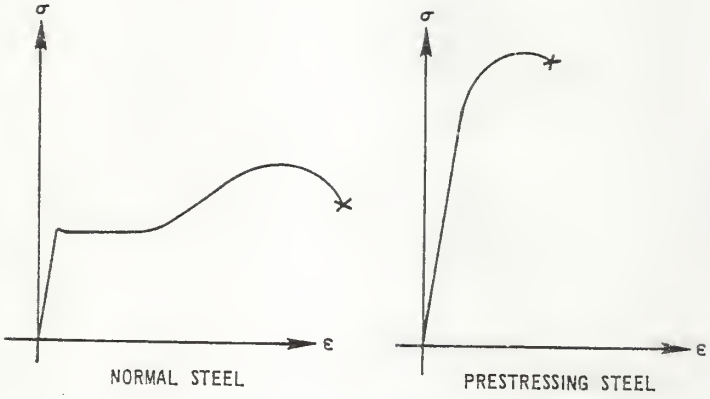

Fig. 3.1 Stress-Strain Curves for Typical Reinforcing Steels

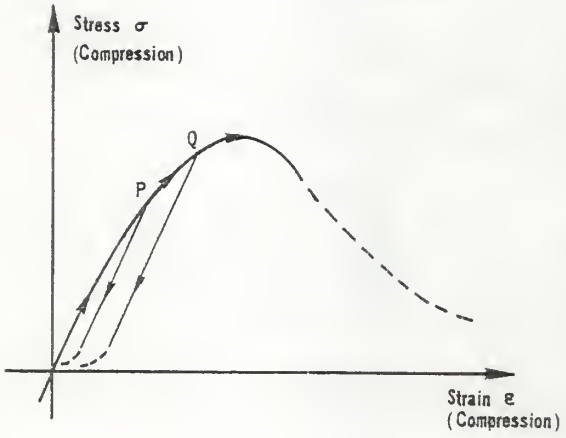

Fig. 3.2 Uniaxial Behavior of Concrete

There is far less information available for biaxial stress states. Most of the biaxial investigations have reported only the ultimate strength of the concrete. However, the most reliable source is probably that of Kupfer, Hilsdorf and Rüsch (15).

The data obtained by Kupfer, Hilsdorf and Rüsch are presented in the form of stress-strain curves. The investigation was based on biaxially loaded specimens tests at different ratios of stress (R) on perpendicular faces. The ratio between the stresses was held constant throughout the loading and nine such ratios were examined covering the entire range of compression-compression, compression-tension, tension-compression and tension-tension. Concrete strength used was approximately 4500 psi for the reported data.

For the requirement of the input data format, each stress-strain curve corresponding to different stress ratios is replaced by a multilinear approximation. As shown in Fig. 3.3, the uniaxial compression stress-strain curve is replaced by linear segments (14), six in this case.

3.1.3 Steel-Concrete Bond

The bond that occurs between the reinforcing bars and the concrete is represented by a model suggested by Ngo and Scordelis (16) (See Fig. 3.4). The normal and tangential bond forces between concrete and the reinforcement are represented by linear or non-linear springs which have

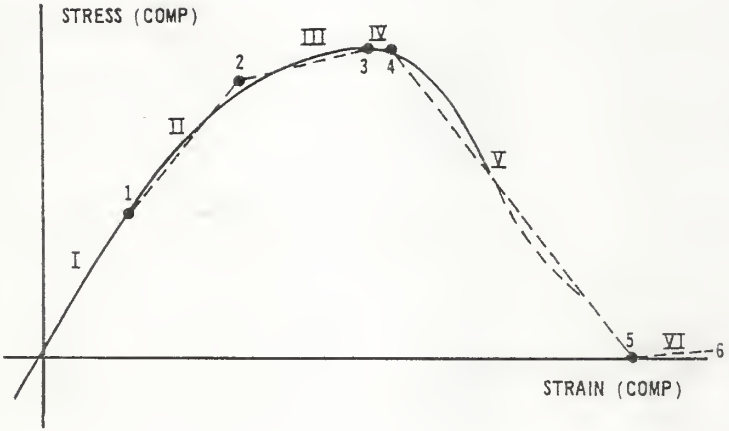

Fig. 3.3 Replacement of Uniaxial Compression Curve With Several (here six) Linear Regions

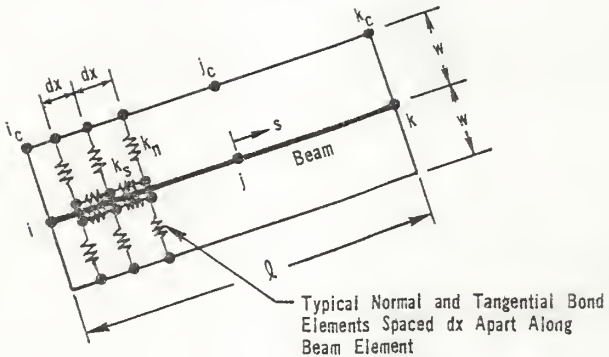

Fig. 3.4 Finite Element Representation of Steel-Concrete Bond

incremental spring constants k_n and k_s, respectively. These springs can be considered as connecting points on the edge of the continuum element with neighboring points on the adjacent "beam" element. Data to be used for k_n and k_s are suggested to follow the cubic bond stress-slip law by Nilson (14,17), or use the uniaxial compression curve of concrete.

3.2 Determination of Damage Levels

It is necessary to define when and how failure occurs in a concrete element.

First, some material property data must be given to the program:

(i) Multilinearlized uniaxial stress-strain information for compression.

(ii) Moduli and Poisson's ratio for each segment (zone) of the multilinearlized compression curve.

(iii) A failure or maximum stress surface which is obtained by applying knowledge and judgment with respect to the materials failure characteristics or by using actual biaxial test information.

A biaxial failure stress plot given by (iii) has the disadvantage of non-uniqueness of strains for any given stress state. For example, given stress data in Fig. 3.3, there is more than one strain at some stress levels. For overcoming this difficulty, the stress plot should be transformed into a strain plot. This transformation is

done by the computer program (14). The result is a biaxial strain plot which has a unique stress for each strain state.

Fig. 3.5 is a strain space damage plot obtained from a stress space damage plot. There are six damage zones in this example, denoted as I, II, III, IV, V and VI. For each damage zone, the zone modulus and Poisson's ratio are given by (ii) and denoted as E_I, ν_I; E_{II}, ν_{II}; ...; E_{VI}, ν_{VI}.

A specimen tested from the zero strain state by increasing the strains ε_1 and ε_2 (Strain 1 and Strain 2 in Fig. 3.5) is assumed to have a particular internal structure with corresponding material properties E_I and ν_I. When the strain state in the test reaches a zone boundary, an instantaneous and incremental change in the internal structure is assumed. Now the material properties are defined as E_{II} and ν_{II} until the next zone boundary is reached. In Fig. 3.5, the move from point R to R_1 has the corresponding material properties E_{II} and ν_{II}, and the move from R_1 to R_2 has the corresponding material properties E_{III} and ν_{III}.

Any move toward the origin is considered to be "unloading" and any move toward the next zone is considered to be a "loading" case. For example, in Fig. 3.5 point P represents the strain state for a concrete element at the end of some increment which is subjected to a change in strain state. Point Q is the predicted next element strain state, i.e., the element strain state moves from P to Q. If point

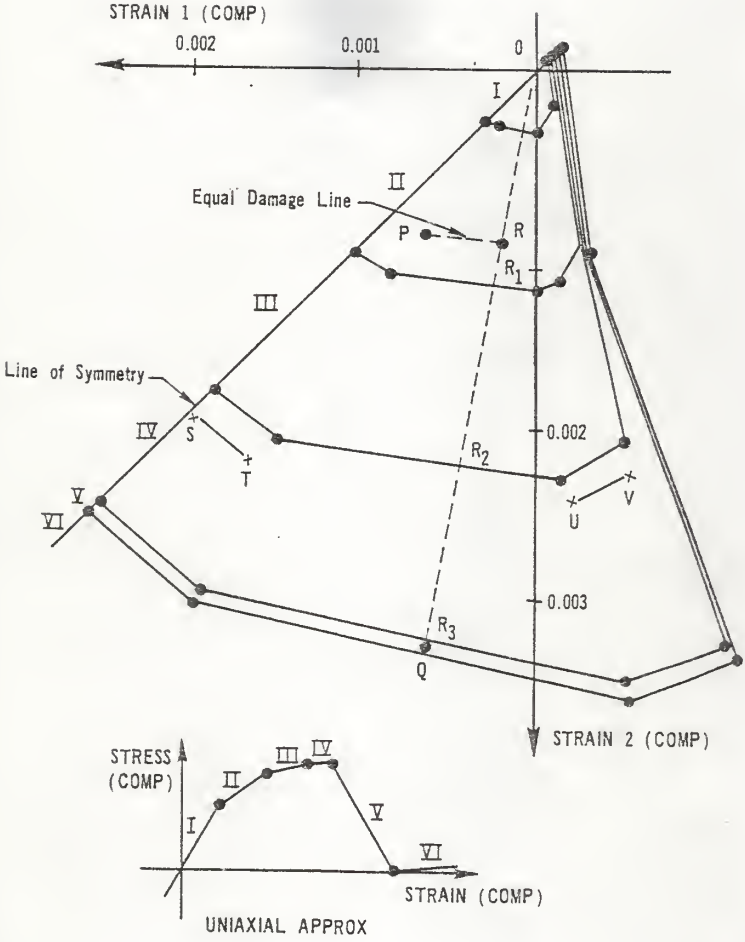

Fig. 3.5 Strain Space Damage Plot

Q lies on a damage level less than or equal to the initial state P, then "unloading" has occurred. If the predicted point Q lies on a greater damage level than P, as shown in Fig. 3.5, then the change defined as "loading" has occurred.

An iterative solution technique is used in the program. It is necessary to be able to predict the incremental values for E and ν when the element is subjected to a change in strain state. As the first approximation for such a prediction as the element strain state moves from P to Q, the following procedure is followed.

First, Q is connected to the origin (OQ in Fig. 3.5), and OQ intersects zone boundaries at R_1, R_2 and R_3 in this example. The equal damage line (line parallel to a zone boundary) which passes through P is drawn and it intersects OQ at R. Now the element strain is assumed to pass from P to Q along P-R-R_1-R_2-R_3-Q. The movement along P-R is a constant damage move which is defined as "unloading" and has properties equal to the initial elastic properties (E_I), according to plasticity theory. The path RQ (RR_1, R_1R_2, R_2R_3) will pass several equal damage zones. So the computation of incrementally estimated values of E are then performed by "weighting" the moduli of the several zones according to the lengths PR, RR_1, R_1R_2, ..., R_nQ, i.e.

$$E = \frac{PR\ E_I + \sum_{i=0}^{n} R_iR_{i+1}\ E_i}{PR + RQ}$$

An exactly similar procedure is used to calculate the incremental value of ν.

3.3 Description of Finite Elements

The finite element method is a computer based technique for obtaining solutions to mechanics problems. In this program, three types of finite elements, i.e., Continuum Element, Reinforcing ("Beam") Element and Bond Element are used.

3.3.1 Continuum Element

For the need of the stress defined cracking criterion, a more accurate displacement behavior element should be used. From among the existing two dimensional finite elements available the quadrilateral element consisting of two linear strain triangles was selected (14,18). Such an element is shown in Fig. 3.6.

For the linear strain triangular sub-element, as shown in Fig. 3.7, the additional three nodes are selected to be located at the mid-points of the sides, and the computer program will compute their coordinates automatically once the corner nodal coordinates are given as input data. The unknowns of the analysis are the nodal displacement $\{\delta\}$ of the element. There are six nodes, and each has two degrees of freedom.

Strains $\{\varepsilon\}$ are expressed in terms of nodal point displacements $\{\delta\}$ through a disolacement transformation matrix $[B]$:

$$\{\varepsilon\} = [B]\{\delta\} \qquad (1)$$

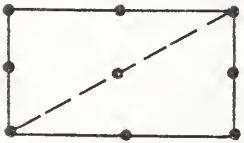

(I + J) – Even

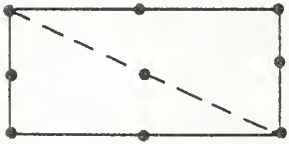

(I + J) – Odd

Fig. 3.6 Quadrilateral Elements I,J is Made Up of Two Triangular Sub-Elements

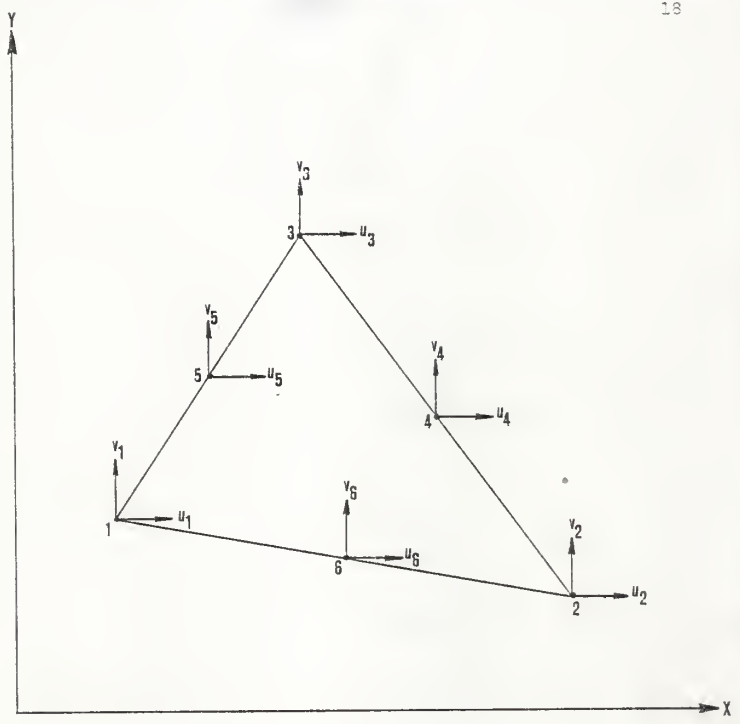

Fig. 3.7 Triangular Sub-Element With Six Nodal Points

Stresses $\{\sigma\}$ are related to strain by a stress-strain law [D], i.e., an elasticity matrix, as

$$\{\sigma\} = [D]\{\varepsilon\} \tag{2}$$

Stresses σ at the edges of the element are replaced by equivalent stress resultants or nodal point forces $\{q\}$ through a force transformation matrix [c]

$$\{q\} = [c]\{\sigma\} \tag{3}$$

By substitution

$$\{q\} = [c]\{\sigma\} = [c][D]\{\varepsilon\} = [c][D][B]\{\delta\} \tag{4}$$

Since the force transformation matrix [c] is equal to the transpose of the displacement transformation matrix [B], the element stiffness matrix [k] can be defined as follows:

$$[k] = [c][D][B] = [B]^T[D][B] \tag{5}$$

and equation (4) can be rewritten in the compact form

$$\{q\} = [k][\delta] \tag{6}$$

The stiffness matrix [K] of the entire system can then be assembled by directly adding the contribution of each individual element stiffness [k] into its proper location.

The resulting equation relates the total loading system $\{Q\}$ and displacements $\{\delta\}$ is:

$$\{Q\} = [K]\{\delta\} \tag{7}$$

For solving the unknown nodal displacements $\{\delta\}$

$$\{\delta\} = [K]^{-1}\{Q\} \tag{8}$$

Once the unknown nodal displacements are computed, then the strains are calculated by Eq. (1), the stresses are calculated by Eq. (2).

3.3.2 Beam Element

The element selected for the bending beam element is a displacement element based upon thick shell theory (14), i.e., a Timoshenko bending element (19), as shown in Fig. 3.8 . This beam element is compatible with the selected continuum element in the previous section. The deflection and rotation of the bending beam element are illustrated in Fig. 3.9 , and this element is one dimensional.

3.3.3 Bond Element

The transfer of stress by bond between concrete and steel is most difficult to model realistically. However, this program adopts a model which has two springs, one acting parallel to the beam axis and one acting perpendicular to it, as shown in Fig. 3.4, which considers the bond between the beam element i-j-k and the side of the adjacent continuum element i_c-j_c-k_c.

For a particular increment of load, express the incremental normal and tangential bond forces (per unit length) between any two adjacent points of the beam element and continuum as

$$B_n(s) = K_n \frac{(u_c - u_b)}{w}$$

$$B_s(s) = K_s \frac{(v_c - v_b)}{w}$$

where

K_n = secant approximation of normal bond modulus

K_s = secant approximation of the tangential bond modulus

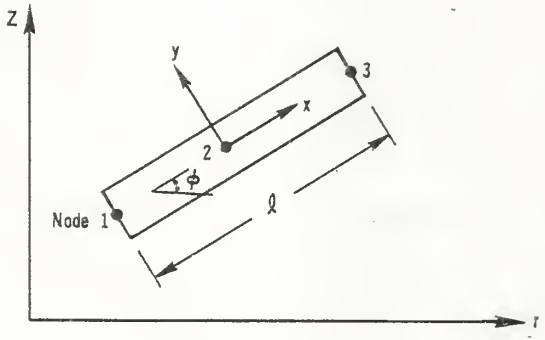

Fig. 3.8 Cross Section of Beam Element

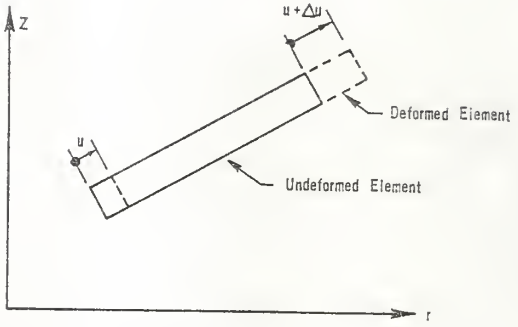

Membrane Displacement

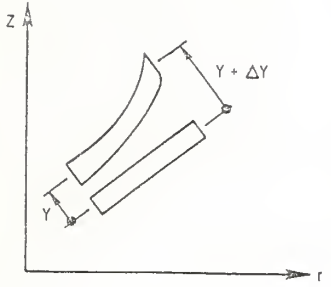

Transverse Displacement

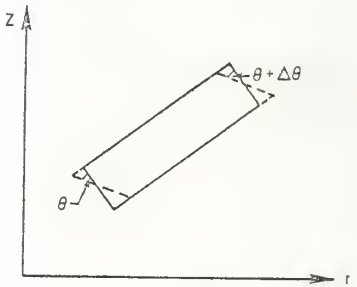

Rotation of Plane Sections

Fig. 3.9 Displacements and Rotation of Beam Element

B_n, B_s = incremental normal and tangential bond forces per unit length

u_b, v_b = incremental beam element displacement in the n and s directions

u_c, v_c = incremental continuum displacements

s = coordinate parallel to beam

n = coordinate normal to beam

w = distance between the center line of the beam element and the edge of the adjacent continuum element

l = length of bending element

3.4 Solution Technique

3.4.1 Linear Analysis

The equation for the unknown nodal displacements $\{\delta\}$ is

$$\{\delta\} = [K]^{-1} \{Q\}$$

The Skyline Equation Solver (20) is used in the program for solving this equation.

3.4.2 Non-linear Analysis and Iteration Procedure

The non-linear analysis procedure is performed by applying loads or specifying boundary displacements in increments and then iterating within each increment to

(i) establish the appropriate incremental material properties by successive comparisons of "secant slope" computations, and

(ii) establish the cracking pattern for the increment.

The iterative analysis within each increment is performed in the following procedure:

1. Each iteration uses "secant properties" (Fig. 3.10) based on an estimated incremental solution.

Start the analysis with estimated strain increments equal to the values at the ends of the first linear portion of the stress-strain plots. Then all the iterations except the first use the strain estimates from the preceding iteration.

2. After each iteration, measure the errors as the differences between the last two secant property predictions divided by the initial or elastic secant value. Compare this measured error with the following criteria.

a) Each element error must be less than a specified maximum.

b) The average of the element errors must be less than a specified maximum.

Iteration is continued until the maximum error criteria are satisfied, then the results of the last iteration are taken as correct.

3. The next increment of load then is applied and the above procedures 1 and 2 are repeated.

A maximum iteration number is input for the problem. The program will terminate if the number of iterations exceeds the maximum specified.

3.4.3 Non-linear Analysis for Cracking Investigation

The strain ray is defined as the length of the line connecting the origin and the predicted strain state in

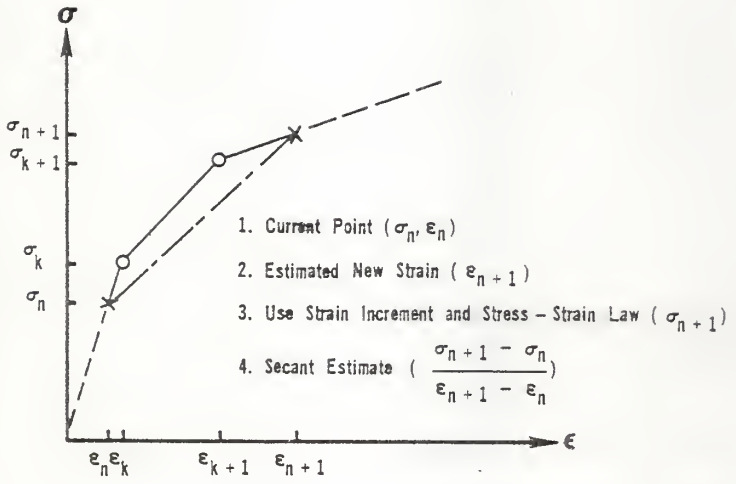

Fig. 3.10 Secant Modulus in Uniaxial Compression

Fig. 3.11. The ratio of the predicted strain ray to the length of the portion of the ray lying within the failure surface is called the "crack ratio" R. Three crack ratios are shown in Fig. 3.11, and when R is ≥1.0, the failure criterion has been exceeded.

The cracks are permitted to form along the finite element grid lines and terminate at "corner node points" (See Fig. 4.1). The decision whether or not neighboring elements should be separated by a crack (i.e., whether the grid line common to the two elements should be permitted to crack) is based on the stress state at their common "side point" (See Fig. 3.12).

The user may specify the initial cracks in the input data, otherwise, after each increment of load is applied to the structure, all side points lying on the boundaries that have not previously cracked will be examined as crack candidates. The crack examination is based on the "cracking ratio". The iteration will continue until there is no longer any tendency to crack and non-linear secant properties have reached the accuracy specified.

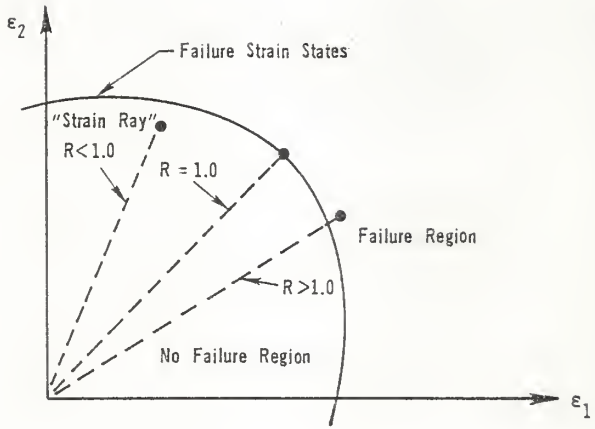

Fig. 3.11 Illustration of Strain Ray Concept

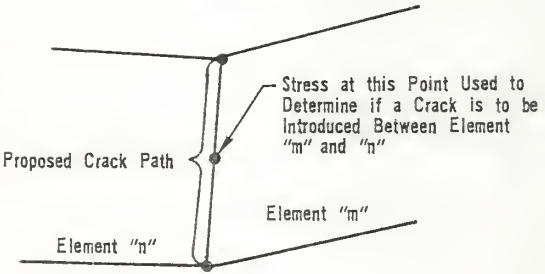

Fig. 3.12 Criterion for Cracking Between Two Elements

CHAPTER IV

USER'S MANUAL OF TAYLOR'S PROGRAM

4.1 Data Input Requirements

Data Input Formats and Explanatory Comments are given here.

4.1.1 Input Formats

A1. Title Card (18A4)

A2. Control Card (I2, 3I1, 3I5, E10.5, 2(E10.5, I5))

Col.				
2	NK	=	0 linear problem 1 non-linear problem	1*
3	NMATBD	=	Number of bond descriptions (See Section A6)	2
4	NMATBM	=	Number of beam geometries (See Section A5)	2
5	NMAT	=	Number of different continuum materials (See Section A4)	2
6-10	IMAX	=	Maximum values of I and J	2,3
11-15	JMAX			
20	ITYPE	=	0 generalized plane stress 1 generalized plane strain 2 axisymmetric analysis	5
21-30	PSV	=	σ_3 for plane stress ϵ_3 for plane strain	6
31-40	PST	=	Thickness of Plane Stress Slab (if left blank the thickness is assumed to be unity)	
41-45	NIT	=	Number of Solution Increments (if left blank it is taken to be unity)	

* See Explanatory Comments in Section 4.1.2.

Col.

46-55 ΔT = Temp. change. This temp. change is used for all nodes except those considered in Section B2.

56-60 NOCRK = Number of grid lines between initiating cracks (if cracking is not to be permitted set NOCRK = -1) 1,7

A3. Iteration Control Card (1X, I4, 2E10.5, 2I5) (This card appears only if NK = 1. See Section A2)

Col.

2-5 ITMAX = Max. no. of iterations allowed in any given increment (failure to converge in this number aborts the problem)

6-15 ERAVGP = The average relative error permitted in the secant modulus for the non-linear elements 8

16-25 ERMAXP = The max. relative error permitted in the secant modulus for the non-linear elements

26-30 IPRNT = The I coordinate of the node at which displacements are printed in each iteration

31-35 JPRNT = The J coordinate of the node at which displacements are printed in each iteration

A4. Continuum Material Cards (repeat Section A4 for each material)

(i) Initial Properties Card (2I5, 6E10.5, I5) 9

5 I = Material Number

10 NON = 0 Linear Isotropic description
1 Linear Anisotropic 3-D description
2 Linear 2-D plane stress or plane strain Anisotropic description
3 Non-linear Isotropic description

Col.

11-20 F_x

21-30 F_y = Body Forces densities in x-y directions

	(Isotropic or initial tangent properties for non-linear material)	(Anisotropic, 3-D)	(Anisotropic 2-D plane stress or plane strain
31-40	E = Modulus	C_{11}	C^*_{11} or C^{**}_{11}
41-50	ν = Poisson's Ratio	C_{12}	C^*_{12} or C^{**}_{12}
51-60	α = Thermal coeff. of expansion	C_{13}	C^*_{13} or C^{**}_{13}
61-70		θ (degrees)	θ (degrees)

75 KA = 0 No initial stress - go to (iii)(i.e., omit card A4ii)

1 Initial stress - card (ii) must follow

(ii) Initial Stress card (4E10.5) (This card is present only if KA = 1, see card A4i)

1-10 σ_{x_o} or σ_{r_o} (Normal initial stress in x or r direction)

11-20 σ_{y_o} or σ_{z_o} (Normal initial stress in y or z direction)

21-30 τ_{xy_o} or τ_{rz_o} (Shearing initial stress)

31-40 σ_{θ_o}

(iii) NON = 0 Go to A4i or A5

NON = 3 Go to A4v

NON = 1 or 2 (Anisotropic material) the following two cards must follow (7E10.5 and 4E10.5)

Col. #	Anisotropic 3-D	Anisotropic 2-D Plane-Stress	Plane Strain
1-10	C_{22}	C^*_{22}	C_{22}^{**}
11-20	C_{23}	C^*_{23}	C_{23}^{**}
21-30	C_{33}	C^*_{33}	C_{33}^{**}
31-40	C_{14}	C^*_{14}	C_{14}^{**}
41-50	C_{24}	C^*_{24}	C_{24}^{**}
51-60	C_{34}	C^*_{34}	C_{34}^{**}
61-70	C_{44}	C^*_{44}	C_{44}^{**}
	(iv)		
1-10	T_1	T^*_1	T_1^{**}
11-20	T_2	T^*_2	T_2^{**}
21-30	T_3	T^*_3	T_3^{**}
31-40	T_4	T^*_4	T_4^{**}

(v) Omit Cards (A4v, vi, vii) unless NON = 3 (2I5)

Col.

1-5 NZ = No. of damage zones

6-10 NORT = No. of stress ratio tests defining the stress-strain surface

(vi) NZ Cards (2E10.5), one for each zone, giving

1-10 ZE = Zone modulus

11-20 ZNU = Zone Poisson's Ratio

(vii) NORT Cards (8E10.3), one for each stress ratio test, giving

Col.

1-10 R = Stress Ratio (Must begin with equal compression-compression, i.e., R = +1 and proceed to compression-tension then tension-tension)

11-20 σ_2ZEJ(I)= Stress at end of 1st zone

21-30 σ_2 " = Stress at end of 2nd zone

. . . . . .

. . . . . .

" " " " NZ "

A5. Beam Cards (1 → NMATBM)(I5, I3, I2, 7E10.5) 10

(i) Initial Properties Card

5 I = Beam number

10 NON = 0 linear material
1 non-linear material

11-20 I = Moment of inertia ($\frac{h^3}{12}$ for cone or strip plate; h = Shell thickness) (A value of zero results in the utilization of an extensional element)

21-30 A = Area (h for cone or strip plate)

31-40 E = Modulus (for non-linear material this is the initial modulus

41-50 α = Thermal coefficient of expansion

51-60 $t_{overlay}$

61-70 α_s = Shear deformation coeff. - if not specified it is set equal to the coefficient for a circular cross-section

71-80 ν = Poisson's Ratio

(ii) (I5) If NON ≠ 1 Omit cards A-5ii and A-5iii

1-5 NZ = Number of segments describing the stress-strain curve

(iii) As many cards (8E10.3) as needed (in fields of ten) to give the pairs of stress-strain values which describe the stress-strain curve, i.e.

1-10 $\sigma(1)$

11-20 $\varepsilon(1)$

21-30 $\sigma(2)$

31-40 $\varepsilon(2)$

etc.

A6. Bond Cards (2I5, 2E10.5)(repeat Section A6 for each bond type) 10

(i) Initial Properties Card

5 NON = 0 Linear properties
1 Non-linear properties

10 I = Bond description No.

11-20 K_n where $F_n = \frac{K_n}{w}(u_{n_c} - u_{n_b})$

21-30 K_s where $F_s = K_s(u_{s_c} - u_{s_b})$ For non-linear properties these are the initial tangent properties

(ii) (2I5) Omit cards A-6ii and A-6iii if NON ≠ 1

1-5 NZN = No. of points defining normal modulus

6-10 NZS = No. of points defining tangent modulus

(iii) As many cards (8E10.3) as needed, using fields of ten, to give pairs of bond stress-bond slip values chosen to describe the bond behavior.

The normal bond curve must be input first followed by the tangetial properties. If either one of these relationships is to be treated elastically no description is required here and the corresponding NZN or NZS value should be input as zero.

1-10 u_1 (Normal or Tangential Stress)

11-20 d_1 (Normal or Tangential Strain)

21-30 u_2 (Normal or Tangential Stress)

31-40 d_2 (Normal or Tangential Strain)

etc.

A7. Node Coordinate Cards (1X, I4, I5, 2E10.5, I5, 2E10.5) 3

2-5 I
6-10 J = Node numbers

11-20 x or r
21-30 y or z = Co-ordinates

35 IGEN = 0 If no points are to be generated between this and previous point
1 If points (along I = Const. or J = Const. line) between this and point specified on the previous card are to be generated

36-45 D = Spacing ratio (if value not specified it is taken to be unity)

46-55 R = Radius of arc connecting points (zero for st. line)

B1. Element Cards (1X, I4, 5I5)(If there are any cards in this group they must be preceded by a card with 1 punched in Col. 1) 4

2-5 I
= Element Coordinates
6-10 J

15 MN = Material Number (0 indicates the absence of material, i.e., a hole)

16-20 NMIS = Number of additional elements for which it is desired to generate material numbers

21-25 INCR
= The amount the element coordinates
26-30 JNCR are to be incremented in the generation procedure

Note: Element Cards need not be used if MN = 1

B2. Temperature Cards (1X, I4, I5, E10.5, 3I5). Corner Node points only (If there are any cards in this group they must be preceded by a card with 2 punched in Col. 1) (Any values specified here supersede the value given on the control card) 4

2-5 I
= Node numbers
6-10 J

11-20 ΔT = value of temperature change at node

21-25 NMIS = Number of additional nodes for which it is desired to generate the same temperature specification

26-30 INCR
= The amount the node numbers are to be
31-35 JNCR incremented in the generation procedure

B3. Boundary Condition Cards (1X, I4, 2(I5, E10.5), E10.5, 2I5, E10.5)(Cards in this group must be preceded by a card with 3 punched in Col. 1) 11

2-5 I
= Node numbers of boundary point
6-10 J

15 IF_1 = 0 if force specified in
1 if displacement 1 dir.

16-25 V_1 = Specified force or displacement in 1 dir.

30 IF_2 = 0 if force specified in
1 if displacement 2 dir.

31-40 V_2 = Specified force or displacement in 2 dir.

41-50 θ = (in degrees) Angle between local and global coordinates

51-55 I'
56-60 J' The above Boundary Conditions are specified for all points (including side points) between and including (I,J) and (I',J'), I, J and I'J' must both be corner points.

61-70 q = Applied uniform surface pressure between I, J and I',J' (when $q \neq c$, then $IF_1 = V_1 = IF_2 = V_2 = \theta = 0$)

B4. Beam Element Description (1X, I4, 7I5). This group of cards must be preceded by a card with 4 punched in Col. 1) 10

2-5 IB
= Node numbers of Beginning of beam
6-10 JB

15 MB = Boundary rotation code for Beginning of beam

0 for $\theta \neq 0$
1 for $\theta = 0$

16-20 IE
= Node numbers of End of Beam
21-25 JE

30 ME = Boundary rotation code for End of beam

0 for $\theta \neq 0$
1 for $\theta = 0$

35 MN = Beam Material Number — See Sections A5 and A6

40 MNBND = Bond Description Number

B5. Beam Intersection Description (1X, I4, 2I5)(This group of cards must be preceded by a card with 5 punched in Col. 1). If no information is given the connection is assumed to be rigid — 10

2-5 I

= Element containing the intersection

6-10 J

15 CODE = 0 if rigidly connected
1 if pin-connected

B6. Definition of Possible Crack Paths (1X, I4, 4I4)(This group of cards must be preceded by a card with 6 punched in Col. 1). If no cards appear in this section all interior element boundaries are possible crack paths. If any possible crack paths are defined in this section then they are the only paths possible. — 4

2-5 I

= Side point located on crack path

6-10 J

11-15 NMIS = Number of additional paths for which it is desired to generate specifications

16-20 INCR

= The amount the node numbers are

21-25 JNCR to be incremented in the generation procedure

B7. Specified Cracks (1X, I4, 3I5)(This group of cards must be preceded by a card with 7 punched in Col. 1).

2-5 I

= Beginning of crack

6-10 J

Crack must begin and end at corner points and lie along a constant I or J line; also I' ≥ I and J' ≥ J

11-15 I'

= End of crack

16-20 J'

B8. Boundary Condition Modification Cards (1X, I4, 2E10.5) Used for increments beyond the first. (Cards in this group must be preceded by a card with 8 punched in Col. 1). 11

2-5	KK	=	Boundary condition number
6-15	V_1	=	Values to replace those previously specified
16-25	V_2		

B9. Incremental Load Card (3E10.3)(This card must be preceded by a card with 9 punched in Col. 1). For each increment (including the first) the following information must be supplied.

1-10	PFBC	=	proportion of	Boundary load or displacement	to be applied in the incr. 11
11-20	PFBF			Body force	
21-30	PFT			Temperature change	

C. For each increment after the first the data sequence is repeated starting with group B7. Any cards in group B7 add to the descriptions previously given; any cards in group B8 modify the information initially given in group B3 (to be used when the modification is not possible simply by using the "Incremental load card").

4.1.2 Explanatory Comments

1. If one or more of the "continuum" materials and/or "beams" and/or "bonds" have a non-linear properties description or if crack generation is permitted (NOCRK $\geq$ 0) the problem is non-linear.

2. As the program is currently dimensioned the following inequalities must be observed:

IMAX $\leq$ 21

JMAX $\leq$ 11

NMAT $\leq$ 3

NMATBM $\leq$ 4

NMATBD $\leq$ 3

No. of Boundary Conditions $\leq$ 99

No. of zones in the continuum stress-strain representation $\leq$ 6

No. of stress ratios in the description of the continuum stress-strain surface $\leq$ 10

No. of zones in the beam stress-strain representation $\leq$ 7

No. of zones in the bond stress-strain representation $\leq$ 9

For changing the dimensions of the program, see Appendix A.

For the sake of economy the I-J grid should be so oriented that JMAX < IMAX since the local bandwidth is determined by the number of J coordinates.

3. Mesh Generation:

The layout and specification of the locations of the node points for a finite element program is often a time-consuming job in which some human error is high. To minimize both effort and error, a subroutine for the nodes generation is used in the program (14) which is based on a method reported by Wilson (21).

The mesh generation is accomplished in the following manner. The coordinates of those nodes whose location are to be exactly defined (the location of all boundary points

must be so specified) are specified by either entering a data card containing the values of I,J and its x and y coordinates or by employing the straight line or circular arc generation options. The location of all other points are calculated by the program.

(a) To lay out a nodal point system for the body to be analyzed, the region of the x-y (r-z) plane containing the body is covered with an array of quadrilaterals. Each vertex of a quadrilateral is called a corner nodal point or corner node, which is identified by an ordered pair of positive integers, denoted by (I,J). Each quadrilateral (or continuum element) is named by the node (I,J) of the lower left hand vertex of the element. Fig. 4.1 illustrates the element (I,J) is defined by the nodes (I,J), (I+1,J), (I,J+1), and (I+1,J+1). In addition to corner nodes, each element has "side nodes" which are located midway along the element edges, i.e., nodes (-(I+1),J), ((I+1), -(J+1)), (-(I+1), (J+1)), (I, -(J+1)). The "side nodes" are not from the input data but determined by the nodes generation subroutine in the program.

(b) The program includes a procedure for generating the coordinates of points intermediate to two specified points. The two specified points and their intermediate points must lie along a constant I or J line. The specification is accomplished by first entering the coordinates of one of the end points followed by the coordinates of the other end point and (i) a code "IGEN". If "IGEN" equals to

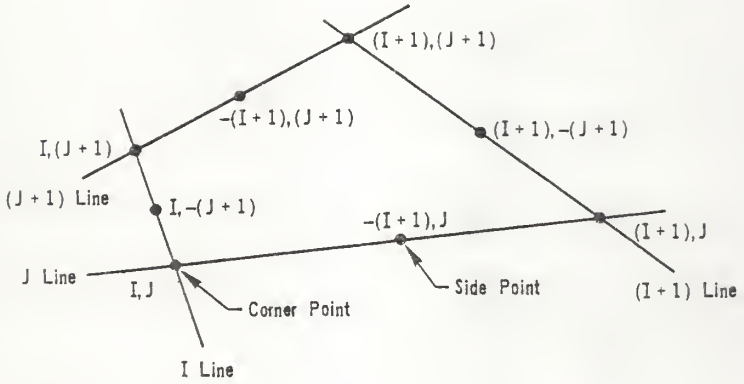

Fig. 4.1 Definition of Element I,J

0 means no points are to be generated between this point and previous point, if IGEN equals to 1 means points (along I = constant, or J = constant line) between this and point specified on the previous card are to be generated. (ii) the spacing ration D and (iii) the arc radius R (this value is left blank for a straight segment). As shown in Fig. 4.2, the operation of generating the points intermediate to the points "a" and "b" is denoted as "a → b" (where point "a" is specified before "b"). The end points for a straight segment may be entered in any order, i.e., the straight line segment shown in Fig. 4.2 may be defined by specifying the end points in order a → b or b → a. However, the circular segments shown in Fig. 4.2 must all be specified a → b. The angle β must not exceed 130°.

The spacing ratio D is equal to the ratio of the lengths of the successive segments, i.e., $D = \frac{\Delta_{n+1}}{\Delta_n}$ in Fig. 4.3. A value of D = 1.0 gives equally spaced points. The location of intermediate points (3.3) and (3.4) in Fig. 4.4 could be generated by either specifying points (3.2)→(3.5) with D = 2.0 or (3.5)→(3.2) with D = 0.5.

(c) The scheme for mesh generation may be thought of as representing a one-to-one mapping from the I-J plane into the x-y plane. Fig. 4.5 illustrates this mapping. The body to be analyzed is shown in Fig. 4.5(A), the points in the I-J plane are shown in Fig. 4.5(B), and their image points in the x-y plane are shown in Fig. 4.5(C). It can

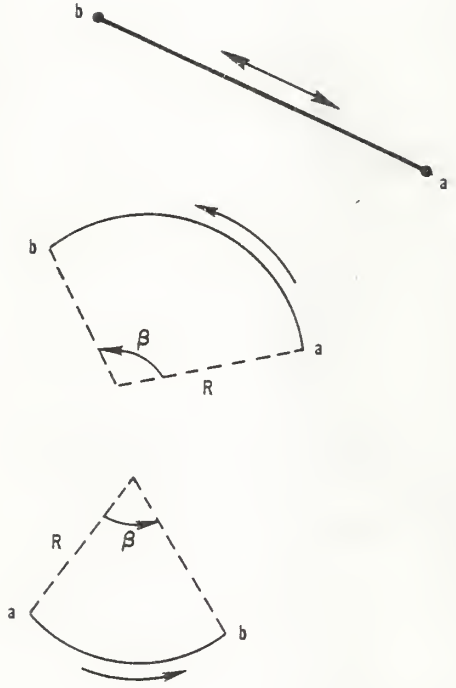

Fig. 4.2 Indicating Required Orders of Specifying End Points a, b for Generation Option

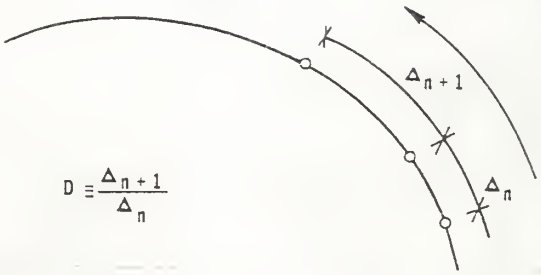

Fig. 4.3 Definition of Spacing Ratio (D)

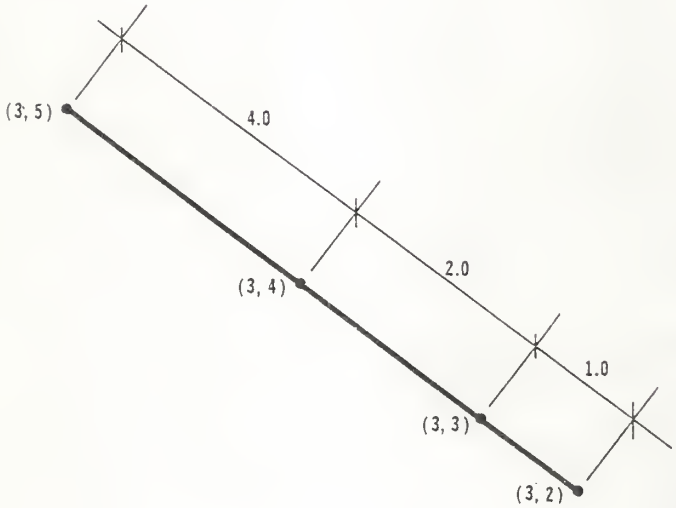

Fig. 4.4 Example of the Straight Line Generation Option

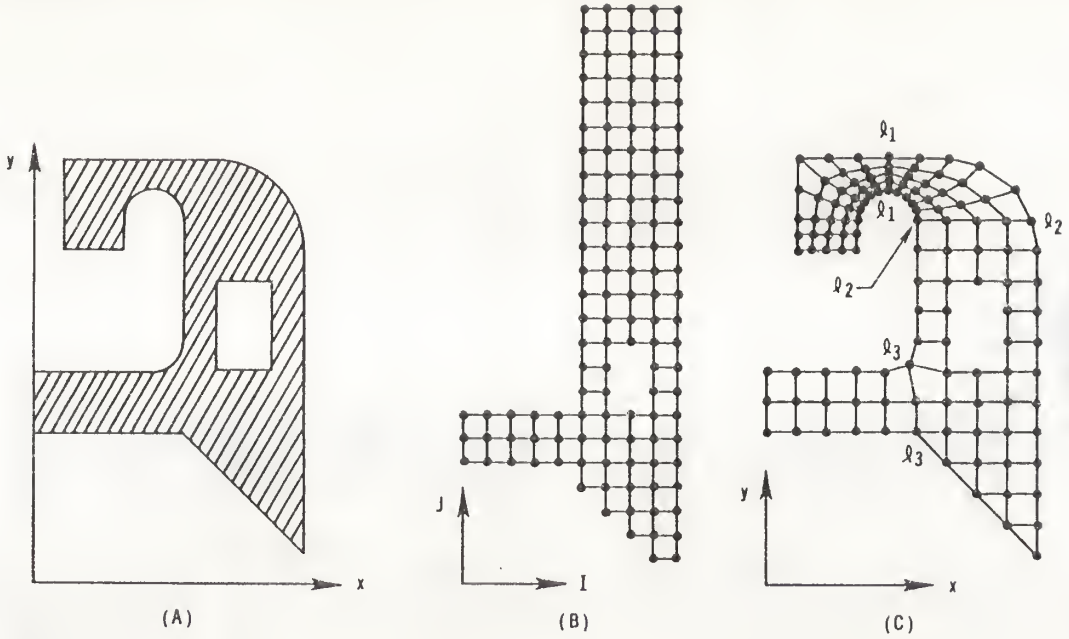

Fig. 4.5 Demonstration Grid (Points Along Lines $_{i}$- $_{j}$ are Specified)

be seen that the inverse images of the quadrilaterals in the x-y plane are squares in the I-J plane. The elements which occupy the "hole" in the body are so indicated by a material number of zero.

(d) Some restrictions were found from the experiences of running this program.

When laying out the nodes for a body, the square elements will give more accurate answers than other types of elements. The vertical strip elements will give more accurate answers than horizontal strip elements.

When the continuum materials are more than one or the two neighboring elements have a big difference in sizes it might effect the bandwidth of the stiffness matrix, then IMAX = 21, JMAX = 11 are no longer correct. IMAX < 21 and JMAX < 11.

After IMAX and JMAX have been decided, all the I lines must have JMAX nodes and all the J lines must have IMAX nodes.

The nodes for a body should start from node (1,1) and be input along the boundary in a counterclockwise direction.

4. The program will assume that the body occupies all the space with a material description number of 1 unless some other number is indicated, i.e., if the elements are holes then a material number of zero must be specified, or if the elements have a material number different from 1 then it has to be specified.

The generation option also permits the specification of the same material number for a sequence of elements with a single card, for example, if the elements (3,2), (3,3), (3,4), (3,5) and (3,6) are all of material Type 3, they could be so specified by assigning the following values:

I = 3
J = 2
MN = 3
NMIS = 4
INCR = 0
JNCR = 1

This generation option can be used in Section (B1), (B2) and (B6) of Input Formats.

5. The program may be used for either plane stress, plane strain or axisymmetric analyses. The bending element for these cases becomes respectively a beam, strip plate or a cone element. For axisymmetric analyses the symbols X-Y-Z in the User's Manual (14) are to be interpreted as R-Z-θ.

6. The value PSV is used to specify a non-zero thickness stress for plane stress analysis, or a non-zero value of normal strain for a plane strain analysis. For axisymmetric analyses this item is to be ignored. The subscript 3 of σ_3 refers to the direction perpendicular to the plane.

7. A crack whose initiation is predicted in a given iteration of a given increment is required to have NOCRK node lines between it and its nearest neighbors.

8. If an error limit is left blank then the criterion is ignored. If more than one criterion is employed then they must all be satisfied before convergence is achieved. For error permitted, see Chapter III.

9. Material Properties:

(a) If the material is linear isotropic, i.e., NON = 0, the material properties are specified by giving values for E (Young's Modulus), ν (Poisson's Ratio), and α (thermal coefficient of expansion).

(b) If the material is linear anisotropic 3-Dimensional description, i.e., NON = 1, then the material properties are specified in terms of the 3-Dimensional elastic constants,

$$\begin{bmatrix} \sigma_1 \\ \sigma_2 \\ \tau_{12} \\ \sigma_3 \end{bmatrix} = \begin{bmatrix} C_{11} & C_{12} & C_{13} & C_{14} \\ C_{12} & C_{22} & C_{23} & C_{24} \\ C_{13} & C_{23} & C_{33} & C_{34} \\ C_{14} & C_{24} & C_{34} & C_{44} \end{bmatrix} \begin{bmatrix} \varepsilon_1 \\ \varepsilon_2 \\ \gamma_{12} \\ \varepsilon_3 \end{bmatrix} + \begin{bmatrix} T_1 \\ T_2 \\ T_3 \\ T_4 \end{bmatrix} \Delta_T$$

(c) If the material is linear 2-Dimensional plane stress (or plane strain) material, i.e., NON = 2, there are two descriptions. For plane stress description,

$$\begin{bmatrix}\sigma_1\\ \sigma_2\\ \tau_{12}\end{bmatrix} = \begin{bmatrix}C_{11}^* & C_{12}^* & C_{13}^*\\ C_{12}^* & C_{22}^* & C_{23}^*\\ C_{13}^* & C_{23}^* & C_{33}^*\end{bmatrix}\begin{bmatrix}\varepsilon_1\\ \varepsilon_2\\ \gamma_{12}\end{bmatrix} + \begin{bmatrix}T_1^*\\ T_2^*\\ T_3^*\end{bmatrix} + \begin{bmatrix}C_{14}^*\\ C_{24}^*\\ C_{34}^*\end{bmatrix}\sigma_3$$

$$\varepsilon_3 = C_{44}^*\,\sigma_3 - C_{14}^*\,\varepsilon_1 - C_{24}^*\,\varepsilon_2 - C_{34}^*\,\gamma_{12} - T_4^*\,\Delta T$$

If PSV = 0 ($\sigma_3 = 0$) one need not specify C_{14}^*, C_{24}^*, C_{34}^*.

For plane strain description,

$$\begin{bmatrix}\varepsilon_1\\ \varepsilon_2\\ \gamma_{12}\end{bmatrix} = \begin{bmatrix}C_{11}^{**} & C_{12}^{**} & C_{13}^{**}\\ C_{12}^{**} & C_{22}^{**} & C_{23}^{**}\\ C_{13}^{**} & C_{23}^{**} & C_{33}^{**}\end{bmatrix}\begin{bmatrix}\sigma_1\\ \sigma_2\\ \tau_{12}\end{bmatrix} + \begin{bmatrix}T_1^{**}\\ T_2^{**}\\ T_3^{**}\end{bmatrix}\Delta T + \begin{bmatrix}C_{14}^{**}\\ C_{24}^{**}\\ C_{34}^{**}\end{bmatrix}\varepsilon_3$$

$$\sigma_3 = C_{14}^{**}\,\varepsilon_1 + C_{24}^{**}\,\varepsilon_2 + C_{34}^{**}\,\gamma_{12} + C_{44}^{**}\,\varepsilon_3 + T_4^{**}\,\Delta T$$

If PSV = 0 ($\varepsilon_3 = 0$) one need not specify C_{14}^{**}, C_{24}^{**}, C_{34}^{**}.

θ is the angle measured counterclockwise between global coordinate system and local coordinate system, as illustrated in Fig. 4.6.

(d) If the material is non-linear description, i.e., NON = 3, the properties are described by (i) uniaxial compression stress-strain curve, (ii) stress strain test data defining the biaxial stress space (See Chapter II).

Linear segments are used for showing the approximate stress-strain curve. As illustrated in Fig. 4.7, there are six damage zones and each zone has zone modulus (E_i) which is the slope of the segment, and Zone Poisson's ratio. The number of damage zones (NZ) is equal to the number of linear segments used to approximate the stress-strain curve.

Figure 4.8 illustrates the Biaxial Stress Data and there are 6 stress ratio testing data sets for the Biaxial Stress Space. Stress Ratios are defined as $R = \sigma_1/\sigma_2$.

The data is given starting with the equal compression-compression case (R = 1.0) and the σ_2 stress at each zone boundary is required. For example, the first card would have R = 1.0, σ_{11}, σ_{21}, σ_{31}, σ_{41}, σ_{51}, σ_{61} (all values of σ_2 along line R = 1.0).

The σ_{ij} (ZEJ(I)) refers here to the value of stress projected on the σ_2 axis at the "i" zone boundary and "j" radial line. The second card may be -0.8, σ_{12}, σ_{22}, σ_{32}, σ_{42}, σ_{52}, σ_{62}, and so on until NZ Zone.

10. Beam Element Properties:

(a) "Beam" elements may only connect "side node points". When viewing a beam element in the I-J plane "side 1" refers to the lower side for a beam element parallel to the I lines and to the right side for a beam element parallel to the J lines. Beams should be located between side points in the grid, the "beginning of beam" gives lower values of (I,J), the "end of beam" gives higher value of (I,J)(See Fig. 4.9).

x'y' = Axes of Anisotropy

xy or rz = Axes of Global Coordinate System

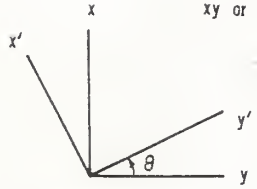

Fig. 4.6

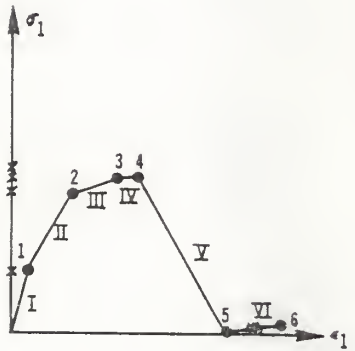

Fig. 4.7

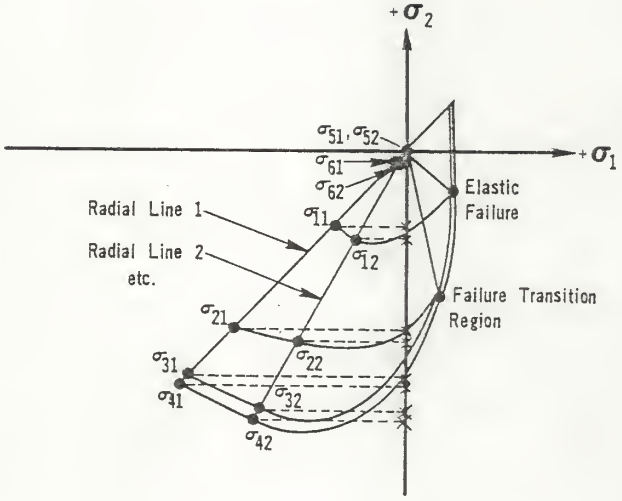
+σ2
+σ1
σ51, σ52
σ61
σ62
σ11
σ12
σ21
σ22
σ31
σ41
σ32
σ42
Radial Line 1
Radial Line 2
etc.
Elastic
Failure
Failure Transition
Region

Fig. 4.8

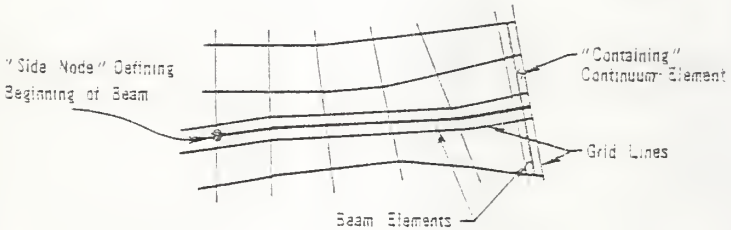
"Side Node" Defining
Beginning of Beam
"Containing"
Continuum Element
Grid Lines
Beam Elements

Fig. 4.9

(b) When beam elements are to be used in conjunction with continuum elements to represent a composite structure (e.g., a reinforced structure) three options are available (See Fig. 4.10).

(i) When a beam element is bonded to the surrounding continuum elements, the thickness of the overlay element is denoted as $t_{overlay}$ (See Fig. 4.10 (i)). The continuum element which overlies the beam element will have the properties defined by its "continuum material cards". The bond elements between the beam element and the surrounding continuum element have properties specified by the "bond cards".

(ii) The beam element may be connected to the surrounding continuum by a bond element by setting the $t_{overlay}$ equal to zero (or specifying the material number of the overlay element to be zero) (Fig. 4.10 (ii)). For example, if it is desired to have a beam on the outside edge of a continuum, then the beam should be located in the outside row of the continuum element and set the $t_{overlay}$ equal to zero.

(iii) If the beam is embedded in the continuum element (Fig. 4.10 (iii)) then giving the "bond description number" (MNBND) as zero and entering the overlay thickness as the negative of its actual value.

(c) Two beams which intersect can have either a rigid or pinned connection. The specification of the type of connection is made in Section B5 of Input Format.

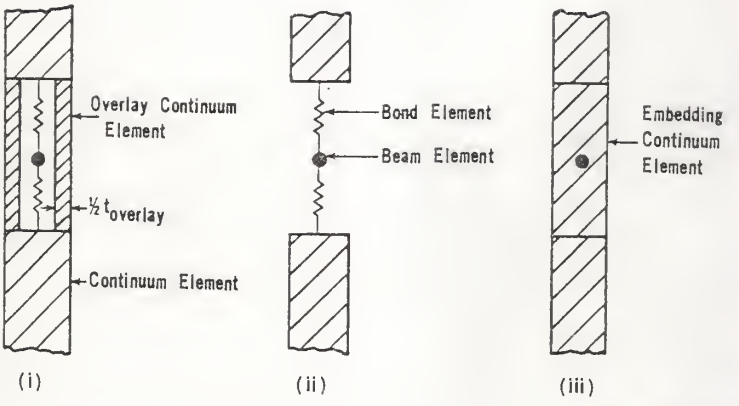

Fig. 4.10 Cross-Section of Possible Beam-Continuum Element Arrangements

(d) For non-linear beam elements and bond elements the stress-strain or bond stress-bond slip curves are described in a piecewise linear fashion. For the bond descriptions the normal properties information should be given followed by the tangential properties information successively for each bond type. Typically, the normal bond characterization may be taken as the uniaxial compression stress-strain diagram for concrete.

11. Boundary Conditions:

(a) Boundary conditions need to be specified for both "side" and "corner" boundary points.

If the boundary conditions are only applied to (I,J) node, then (I',J') = (0,0). If the boundary conditions

are applied to all the points (including side points) between and including (I,J) and (I',J'), then (I',J') is not equal to zero. The points (I,J) and (I',J') must both lie on a constant I or J line.

The pressure q may be applied to a continuum surface or directly to a beam. A positive value of pressure q is defined as the body under compression. If the pressure is specified from (I,J) to (I',J'), it must be specified counterclockwise along the boundary of the body. Pressure specifications must precede any other specification related to the same boundary points. When $q \neq 0$, then $IF_1 = IF_2 = V_1 = V_2 = \theta = 0$. In Fig. 4.11, "θ" is the angle measured counterclockwise from the global coordinate system (x-y) to the local coordinate system (1-2).

(I,J) and (I',J') both must be corner points. The only exception is when uniform pressure is applied to a "beam", then they would be side points.

(b) The specification of "increments of boundary conditions" (Section B9 of Input Formats) may involve a) Boundary loads or displacements (value V_1, V_2 or q in Section B3), b) Body forces (value F_x or F_y in Section A4) and c) Temperature change (value ΔT in Section B2).

(i) The quantities of the first increment of the boundary conditions are the original values specified in card (B3), (A4) and (B2) times the values specified in card (B9). Then the next increment of the boundary conditions will be the values of (B9)

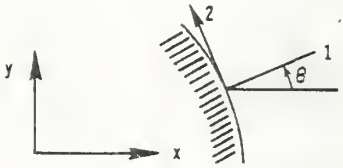

Fig. 4.11

times the original values specified in (B2), (A4) and (B2) added to the sum of the previous boundary conditions. For example,

(B3) Card 1: $V_1 = 0.7$

(B9) Card 1: 9 (Control Card)
Card 2: PFBC = 5.0
Card 3: 9 (Control Card)
Card 4: PFBC = 6.0

then,

Increment 1 : $V_1 = 0.7 \times 5.0 = 3.5$

Increment 2 : $V_1 = 0.7 \times 6.0 + 3.5 = 7.7$

(ii) Non-proportionate boundary loads or displacements may be specified by modifying, in any given increment, the values of V_1 and V_2 specified in Section B3. This modification is carried out by entering cards in B8. Values once entered into B8 modify the original values specified in B3, then these values will be used for all subsequent increments until they are modified again by the use of B9.

The "Boundary Condition Numbers" (KK) in B8 are the sequence numbers of boundary conditions specified in B3 and are printed with the boundary condition information.

4.2 Output

The output of the program consist of:

1. A statement of the input

2. For each increment:

a) The number of iterations necessary to achieve a solution

b) The locations of newly formed cracks

c) For each node in the system the stresses, strains and displacements are printed. When a crack runs through a node point multiple states of stress, strain and displacement exist. These multiple values are printed for each of the subpoints in the order shown below.

For Corner Node Points

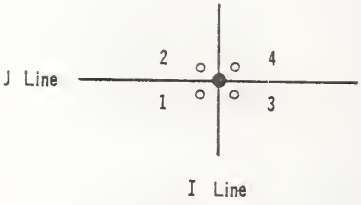

For Side Node Points

or

Several examples of the subpoints for which print out would be given are shown below.

i)

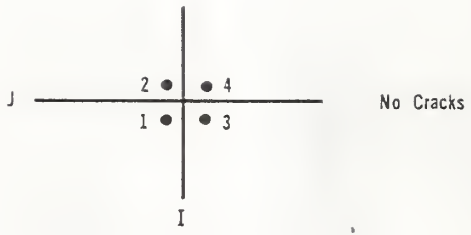

Print out is given only for Subpoint 1 as the other points have the same values.

(ii)

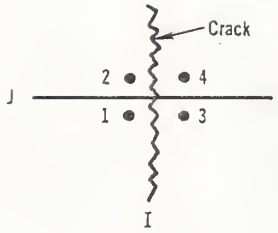

Print out given for Subpoints 1 and 3 (Point 2 has the same values as 1 and 4 same as 3).

(iii)

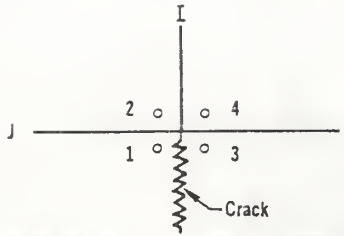

Print-out Given Only for Point 1 as All Four Points Represent the Tip of the Crack

(iv)

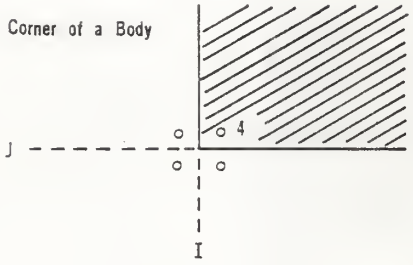

Print-out Given Under the Label of Subpoint 4

d) For side points which have beam (strip plate or cone) elements passing through them information concerning the forces and moments in the beam element and the bond forces between the element and the surrounding contimuum is given:

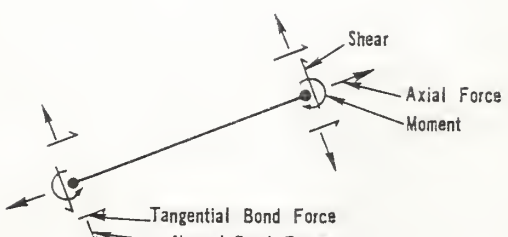

Definition of Non-self-evident Output Headings

F-X (etc)	Body force in X-direction per unit of volume
NU	Poisson's ratio
ALPHA	Thermal coefficient of linear expansion
S.C.F.	Timoshenko shear coefficient
PO	Subpoint number
U, V	Continuum displacements in X(R) and Y(Z) directions
E-X (etc)	Strain in X (radial) direction
S-X (etc)	Stress in X (radial) direction
S-1	Most tensile principal stress
TH	Angle between S1 and X-axis in degrees
U, Y	Tangential and transverse displacement components for a bending element
P, V, M	Axial force, shearing force and bending moment in bending element
PZ (ORPH)	Force in Z-direction (Place Strain) Force in hoop direction (Axisymmetric)
SBN1, SBS1	Normal and tangential bond force quantities for side 1 of beam.

CHAPTER V

NUMERICAL EXAMPLES

Some numerical examples are presented in this chapter to explain the techniques used for modelling the structural elements and to show how the computer program works.

5.1 W Shape Steel Beam Without Web Openings

A simply supported W shape 18 x 50 steel beam with 132" span length subject to 10 kips concentrate load at midspan was used here. Techniques were used for modelling and analyzing this beam (elastic behavior only).

5.1.1 Simplification of the Problem

(A) Since there is no interest in the stresses throughout the entire beam, the portion of interest can be analyzed by considering two cutting sections (Fig. 5.1). The moments and shear forces on the free body in Fig. 5.1 (b) could not be input to the program directly. These moment and shear were approximated by a series of concentrated loads applied at the nodal points on the end sections. The bending stresses at the end sections were calculated by the simple beam theory

$$\sigma = \frac{My}{I}$$

This stress distribution is linear along the boundary. The formulas of calculating the nodal forces are: (See Fig. 5.2)

$$P_1 = \frac{Lt}{6} (2 p_1 + p_2)$$

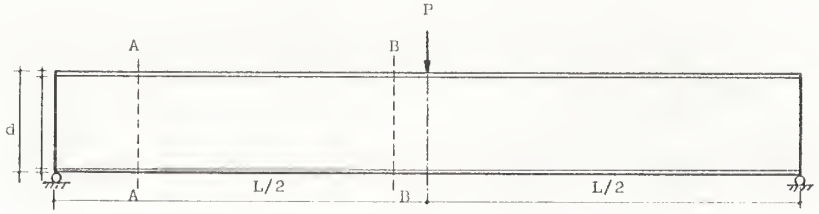

(a)

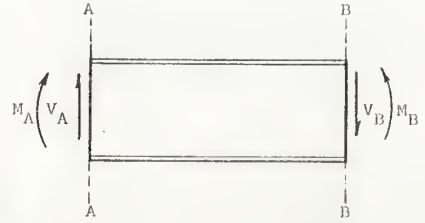

(b)

Fig. 5.1

$$P_2 = \frac{Lt}{6}(2\,p_2 + p_1)$$

P_i = nodal force, i=1, 2

p_i = force intensity per unit area, i=1, 2

t = thickness

The concentrated load at each nodal point is the sum of the resultants from the adjacent sides.

The shear stresses at the end section are calculated by

$$\tau = \frac{VQ}{I_b}$$

The half section of a beam is shown in Fig. 5.3 when $0 \le y \le d/2 - t_f$

$$Q = b_f t_f \left(\frac{d}{2} - \frac{t_f}{2}\right) + t_w \left(\frac{d}{2} - t_f - y\right)\left(\frac{\frac{d}{2} - t_f}{2} + \frac{y}{2}\right)$$

$$= Q_F + Q_w(y)$$

$$\therefore \tau = \frac{V}{I\,t_w}\left[Q_F + Q_w(y)\right]$$

The area of shear stress diagram A_i is:

$$A_i = \int_0^{\xi_i} \tau\, t_w dy - \sum_{j=1}^{i-1} A_j, \quad i=2, n$$

where

$$\xi_i = \frac{1}{2}(y_{i+1} + y_i), \quad 1 \le i \le n-1$$

$$\xi_n = y_n$$

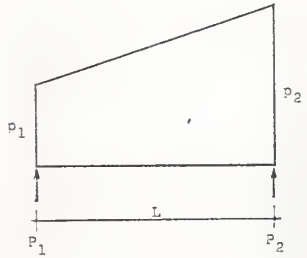
p1
p2
L
P1
P2

Fig. 5.2

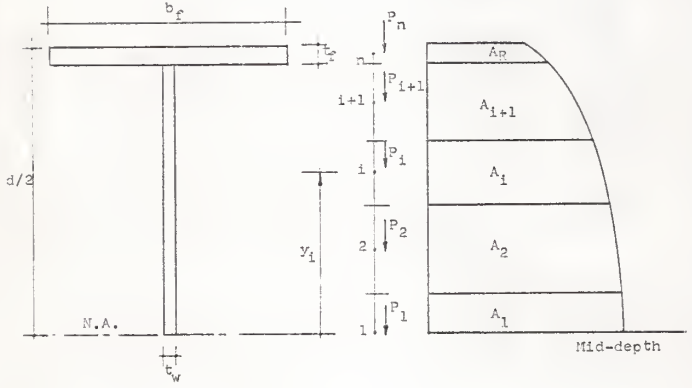
bf
tf
d/2
N.A.
tw
yi
Pn
n
Pi+1
i+1
Pi
i
P2
2
P1
1
An
Ai+1
Ai
A2
A1
Mid-depth

Fig. 5.3

and

$$\int_0^{\xi_i} \tau\, t_w d_y = \frac{V}{I} \int_0^{\xi_i} (Q_F + Q_W)\, dy$$

$$= \frac{V}{I} \{b_f t_f (\frac{d}{2} - \frac{t_f}{2})\, \xi_i + \frac{1}{2}\, t_w\, [(\frac{d}{2} - t_f)^2\, \xi_i$$

$$- \frac{1}{3}\, \xi_i{}^3]\}$$

$$\therefore A_i = \frac{V}{2I}\, \xi_i\, \{b_f t_f\, (d - t_f) + t_w\, [(\frac{d}{2} - t_f)^2 - \frac{1}{3}\, \xi_i{}^2]\}$$

$$- \sum_{j=1}^{i-1} A_j,\ i=1,\ n$$

where I is the moment of inertia, V is shear force at end section.

The concentrated shear force at each nodal point P_i is the area of shear stress diagram A_i (for $i \neq 1$), and $P_1 = 2\, A_1$.

(B) Modify the flange thickness to be the web thickness for a W shape beam.

In using the plane stress finite element method for analysis, the three-dimensional structure with different thicknesses has to be modified to a two-dimensional structure with the same thickness.

The stiffness matrix of a triangular element for the plane stress analysis is defined by:

$$[k] = \begin{bmatrix} K_{ii} & K_{ij} & K_{im} \\ K_{ji} & K_{jj} & K_{jm} \\ K_{mi} & K_{mj} & K_{mm} \end{bmatrix}$$

where i, j, m are the three nodes of the triangular element and each element of matrix [k] is a 2 x 2 matrix given by the general expression

$$[K_{ij}] = \{B_i\}^T [D]\{B_j\} \cdot t \cdot \text{area}$$

The matrix {B} is the displacement-strain matrix whose elements are independent of the coordinates X, Y of the system. [D] is the elasticity stress matrix which has the expression

$$[D] = \frac{E}{1-\nu^2} \begin{bmatrix} 1 & \nu & 0 \\ \nu & 1 & 0 \\ 0 & 0 & \frac{1-\nu}{2} \end{bmatrix}$$

where ν is the Poisson's ratio and E is Young's modulus.

The equation $[K_{ij}]$ becomes to

$$[K_{ij}] = \{B_i\}^T \left(\frac{Et}{1-\nu^2}\right) \begin{bmatrix} 1 & \nu & 0 \\ \nu & 1 & 0 \\ 0 & 0 & \frac{1-\nu}{2} \end{bmatrix} \{B_j\} \cdot \text{area}$$

The "Et" value is a constant for a plane stress analysis and E can be modified in order to use the flange thickness equal to the web thickness.

(C) Equivalent reinforcing ("beam") elements for flanges.

Another way of modifying the three-dimensional structure with different thicknesses to the two-dimensional structure was followed. Equivalent "beam" elements were used for the flanges and were bonded to the continuum element (web) with bond elements. These beam elements have one-dimensional material properties and can transfer axial forces, shear forces and bending moments.

5.1.2 Numerical Examples

Problem 1: Half of the W18x50 steel beam. Fig. 5.4 shows the discretization of the analyzed portion. The flanges of the beam were treated as equivalent reinforcing bars ("beam elements"). The computer results are given in Table 5.1 and are compared with simple beam theory.

Problem 2: Fig. 5.5 shows the discretization of the W18x50 steel beam by modifying the flange thickness to be the web thickness (Section 5.1.1 (B)). Table 5.2 gives the results of the computer program.

Problem 3: Fig. 5.6 shows the discretization of the W18x50 steel beam by using the cutting sections (Section 5.1.1 (A)) and equivalent reinforcing elements techniques (Section 5.1.1 (C)). Table 5.3 gives the results of the computer program.

5.2 W Shape Steel Beam With Web Openings

The cutting sections technique in Section 5.1 was also used in this type of problem. For the elastic

W18x50 Beam

IMAX = 21 $E_s = 29 \times 10^3$ ksi

JMAX = 8 $\nu_s = 0.3$

1 inch = 2.54 cm $f_y = 36$ ksi

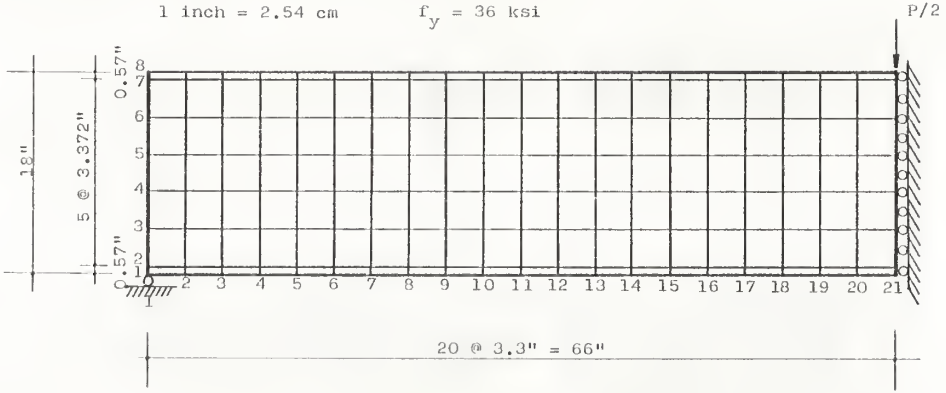

Fig. 5.4 Discretization of Problem 1

Table 5.1 Results of Problem 1, stress (ksi),
1 ksi = 6.9 MN/m^2

Node (I,J)	Beam Theory σ_x	Computer Output σ_x	Error (%)	Node (I,J)	Beam Theory σ_x	Computer Output σ_x	Error (%)
(11,1)	1.8516			(16,1)	2.7774		
(11,-2)	1.7930	1.7780	0.8%	(16,-2)	2.6895	2.6994	0.4%
(11,2)	1.7344	1.78	2.6%	(16,2)	2.6015	2.70	3.8%
(11,-3)	1.3875	1.42	2.3%	(16,-3)	2.0812	2.16	3.8%
(11,3)	1.0406	1.06	1.9%	(16,3)	1.5609	1.62	3.8%
(11,-4)	0.6937	0.704	1.5%	(16,-4)	1.0406	1.08	3.8%
(11,4)	0.3469	0.348	0.3%	(16,4)	0.5203	0.541	4.0%
(11,-5)	0.0000	7.79×10^{-3}	-	(16,-5)	0.0000	3.57×10^{-4}	-
(11,5)	-0.3469	-0.363	4.6%	(16,5)	-0.5203	-0.540	3.8%
(11,-6)	-0.6937	-0.716	3.2%	(16,-6)	-1.0406	-1,08	3.8%
(11,6)	-1.0406	-1.07	2.8%	(16,6)	-1.5609	-1.62	3.8%
(11,-7)	-1.3875	-1.42	2.3%	(16,-7)	-2.0812	-2.16	3.8%
(11,7)	-1.7344	-1.77	2.0%	(16.7)	-2.6015	-2.70	3.8%
(11,-8)	-1.7930	-1.7719	1.2%	(16,-8)	-2.6895	-2.6994	3.7%
(11,8)	-1.8516			(16,8)	-2.7774		

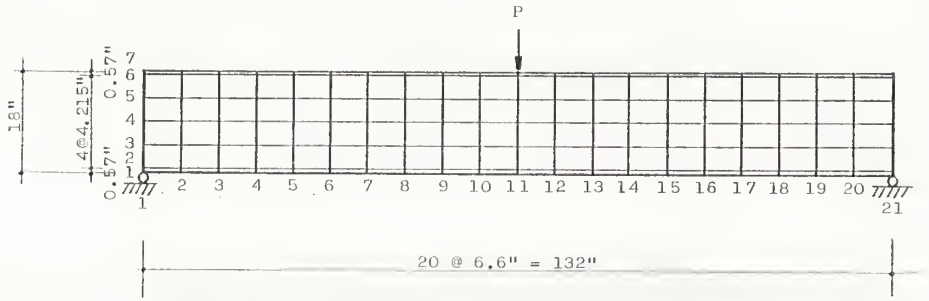

W18x50 Beam

IMAX = 21 $E_s = 29 \times 10^3$ ksi

JMAX = 7 $\nu_s = 0.3$

1 inch = 2.54 cm $f_y = 36$ ksi

Fig. 5.5 Discretization of Problem 2

Table 5.2 Results of Problem 2, stress (ksi),
1 ksi = 6.9 MN/m^2

Node (I,J)	Beam Theory σ_x	Computer Output σ_x	Node (I,J)	Beam Theory σ_x	Computer Output σ_x
(16,1)	1.852	3.179	(9,1)	2.963	4.868
(16,-2)	1.793	3.074	(9,-2)	2.869	4.572
(16,2)	1.734	1.557	(9,2)	2.775	2.372
(16,-3)	1.301	2.24	(9,-3)	2.081	3.37
(16,3)	0.867	1.47	(9,3)	1.387	2.16
(16,-4)	0.434	0.721	(9,-4)	0.694	0.984
(16,4)	0.000	-2.86×10^{-2}	(9,4)	0.000	-1.69×10^{-1}
(16,-5)	-0.434	-0.768	(9,-5)	-0.694	-1.32
(16,5)	-0.867	-1.50	(9,5)	-1.387	-2.45
(16,-6)	-1.301	-2.24	(9,-6)	-2.081	-3.46
(16,6)	-1.734	-1.551	(9,6)	-2.775	-2.320
(16,-7)	-1.793	-3.069	(9,-7)	-2.869	-4.554
(16,7)	-1.852	-3.174	(9,7)	-2.963	-4.687

W18x50 Beam

IMAX = 21 $E_s = 29 \times 10^3$ ksi

JMAX = 9 $\nu_s = 0.3$

1 inch = 2.54 cm $f_y = 36$ ksi

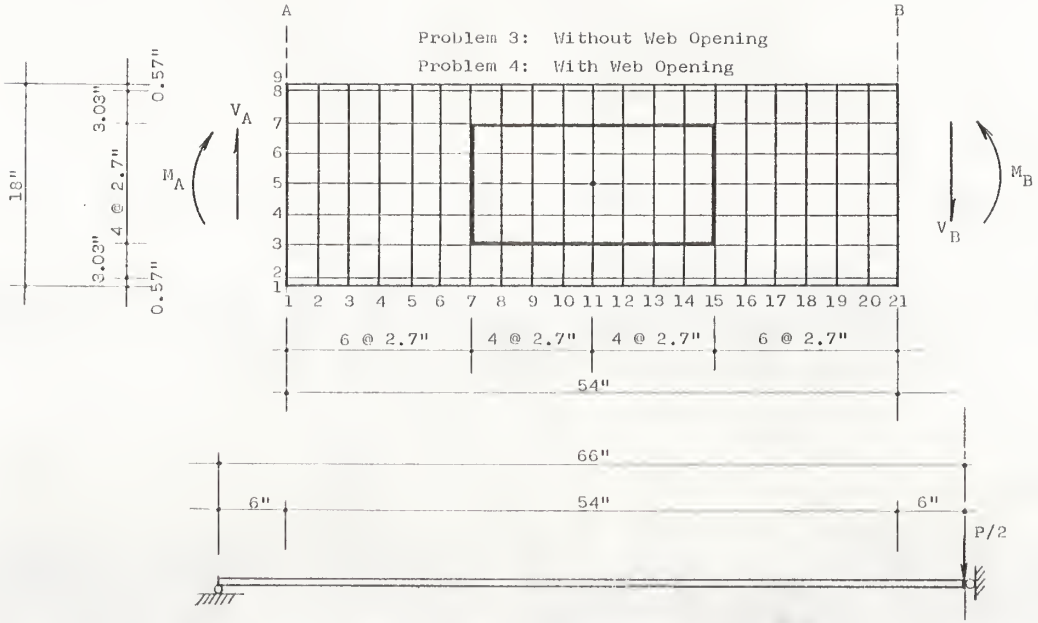

Table 5.3 Results of Problem 3, stress (ksi),
1 ksi = 6.9 MN/m^2

Node (I,J)	Beam Theory σ_x	Computer Output σ_x	Error (%)	Node (I,J)	Beam Theory σ_x	Computer Output σ_x	Error (%)
(7,1)	1.2456			(11,1)	1.8516		
(7,-2)	1.2062	1.1799	2.2%	(11,-2)	1.7929	1.7881	0.3%
(7,2)	1.1667	1.18	1.1%	(11,2)	1.7344	1.79	3.2%
(7,-3)	0.9571	0.971	1.5%	(11,-3)	1.4227	1.47	3.3%
(7,3)	0.7474	0.76	1.7%	(11,3)	1.1111	1.15	3.5%
(7,-4)	0.5605	0.571	1.3%	(11,-4)	0.8332	0.859	3.1%
(7,4)	0.3737	0.381	2.0%	(11,4)	0.5555	0.573	3.2%
(7,-5)	0.1868	0.191	2.2%	(11,-5)	0.2777	0.286	3.0%
(7,5)	0.0	-9.31×10^{-5}	-	(11,5)	0.0000	1.72×10^{-4}	-
(7,-6)	-0.1868	-0.191	2.2%	(11,-6)	-0.2777	-0.287	3.3%
(7,6)	-0.3737	-0.381	2.0%	(11,6)	-0.5555	-0.573	3.2%
(7,-7)	-0.5605	-0.571	1.3%	(11,-7)	-0.8332	-0.859	3.1%
(7,7)	-0.7474	-0.571	1.7%	(11,7)	-1.1111	-1.15	3.5%
(7,-8)	-0.9571	-0.971	1.5%	(11,-8)	-1.4227	-1.47	3.3%
(7,8)	-1.1667	-1.18	1.1%	(11,8)	-1.7344	-1.79	3.2%
(7,-9)	-1.2062	-1.1813	2.1%	(11,-9)	-1.7929	-1.7890	0.2%
(7,9)	-1.2456			(11,9)	-1.8516		

analysis, the Vierendeel Analysis was used to predict the stresses around the web openings and check with the output of the computer program.

5.2.1 Vierendeel Analysis

The basic assumption of the analogy is that secondary moments caused by shearing forces in the region of the hole are zero at midlength of the hole. Final stresses may be obtained by considering stresses due to the primary bending moment using the net section and adding to these the stresses due to the secondary bending moment using the T-section above and below the opening.

First, consider the moment M_p which causes the basic bending stresses σ_p at the centerline of the opening (See Fig. 5.7 (a).

$$\sigma_p = \pm \frac{M_p y}{I_n}$$

where I_n = moment of inertia of the net beam about its centroidal axis, and y = the transverse distance from the centroidal axis of the net beam. Thus, M_p is assumed to be carried by the reduced section at the hole acting according to elementary beam theory.

The secondary moment M_s caused by shear introduces the secondary bending stresses, σ_s. In Fig. 5.7 (b), the hole is symmetrical with respect to the horizontal axis of symmetry of the beam.

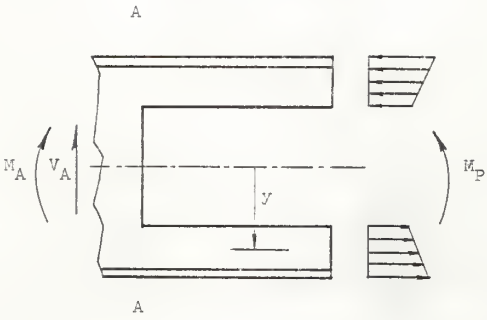

(a)

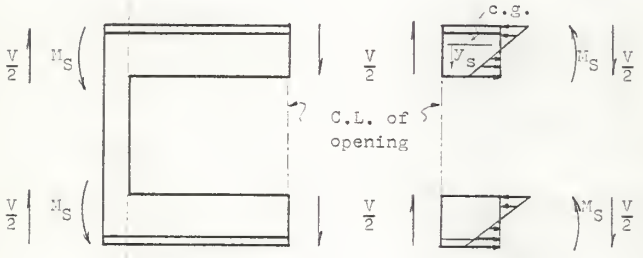

(b)

Fig. 5.7 Vierendeel Analysis

$$\sigma_s = \pm \frac{M_s y_s}{I_{cg}}$$

where I_{cg} = the moment of inertia of the top or bottom section about its centroid, y_s = the transverse distance from the centroid of the top or bottom section.

So, the stress σ at any section is

$$\sigma = \sigma_p + \sigma_s$$

$$= \pm \frac{M_n y}{I_n} \pm \frac{M_s y_s}{I_{cg}}$$

5.2.2 Numerical Example

Problem 4: Fig. 5.6 also gives the discretization for the analyzed portion of a W18x50 steel beam with a web opening by assuming elements I from 7 to 15, J from 3 to 6 have the material properties equal to zero. Table 5.4 shows the results of the computer output which is compared with the results from the Vierendeel Analysis.

5.3 Composite Steel-Concrete Beam Without Web Openings

Problem 5: A W shape 18x50 steel beam with 4" thick concrete slab on top was taken for an example. Fig. 5.8 shows the discretization of half of the beam without an opening. The beam was described as two materials. The flanges were treated as reinforcing bars as explained in Section 5.1.1 (C). The thickness of the concrete slab was

Table 5.4 Results of Problem 4, stress (ksi)
1 ksi = 6.9 MN/m^2

Node (I,J)	Vierendeel Method σ_x	Computer Output σ_x	Node (I,J)	Vierendeel Method σ_x	Computer Output σ_x	Node (I,J)	Vierendeel Method σ_x	Computer Output σ_x
(7,1)	- 5.9832		(11,1)	1.9426		(15,1)		
(7,-2)	- 1.3589	-0.5685	(11,-2)	1.9811	1.8655	(15,-2)	5.1205	4.3129
(7,2)	0.6529	-2.01	(11,2)	1.8196	1.87	(15,2)	2.9863	5.82
(7,-3)	11.344	7.88	(11,-3)	1.4926	1.63	(15,-3)	- 8.3590	-4.81
(7,3)	22.035	17.5	(11,3)	1.1656	1.40	(15,3)	-19.7042	-15.6
(7,-4)		1.88	(11,-4)			(15,-4)		-1.73
(7,4)		-0.6	(11,4)			(15,4)		0.542
(7,-5)		-0.522	(11,-5)			(15,-5)		0.492
(7,5)		1.78×10^{-4}	(11,5)			(15,5)		-3.32×10^{-4}
(7,-6)		0.523	(11,-6)			(15,-6)		0.492
(7,6)		0.6	(11,6)			(15,6)		-0.542
(7,-7)		-1.88	(11,-7)			(15,-7)		1.73
(7,7)	-22.035	-17.5	(11,7)	-1.1656	-1.40	(15,7)	19.7042	15.6
(7,-8)	-11.344	-7.88	(11,-8)	-1.4926	-1.64	(15,-8)	8.3590	4.81
(7.8)	- 0.6529	2.0	(11,8)	-1.8196	-1.87	(15,8)	- 2.9863	-5.82
(7,-9)	1.3589	0.5662	(11,-9)	-1.8811	-1.8662	(15,-9)	- 5.1205	-4.3129
(7,9)	5.9832		(11,9)			(15,9)		

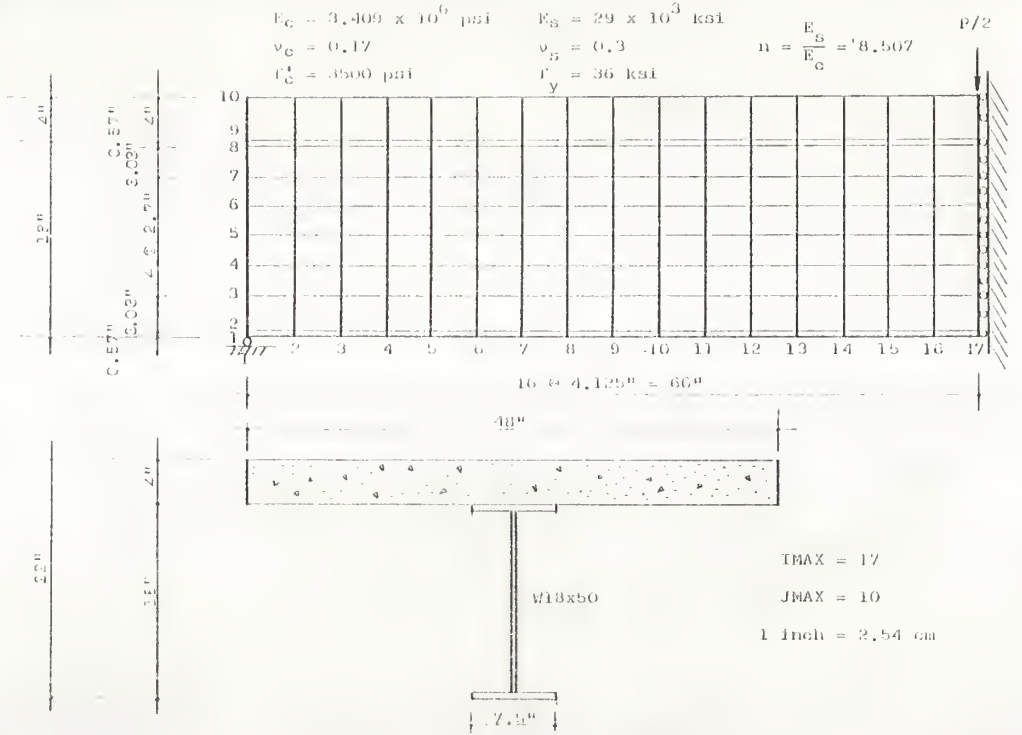

Fig. 5.8 Discretization of Problem 5

modified into a thickness corresponding to the steel web by using Section 5.1.1 (B).

The results from the computer output were checked by beam theory in which the concrete slab was transformed to an equivalent steel block. Table 5.5 gives these results.

5.4 Composite Steel-Concrete Beam With Web Openings

Problem 6: Using the same beam as Problem 5 by assuming the material properties of the elements which covered by the hole equal to zero. Fig. 5.9 shows the discretization of the beam. Table 5.6 gives the results and they were checked by Vierendeel Analysis.

5.5 Reinforced Concrete Beam - Non-linear Analysis

5.5.1 Problem 7: A simply supported concrete beam with four No. 8 reinforcing bars was analyzed here. The loads were applied in three increments resulting in 9^{k}, 24^{k} and 36^{k} total force which were symmetrical about the centerline of the beam length.

A sketch of the half of this beam and the discretization of analyzed portion are shown in Fig. 5.10, the thickness of the beam is 10".

For the concrete properties, a non-linear uniaxial compression stress-strain (σ-ε) curve was assumed to be a parabola by the following equation

$$\sigma = f'_c \left[2 \left(\frac{\varepsilon}{\varepsilon_o}\right) - \left(\frac{\varepsilon}{\varepsilon_o}\right)^2\right]$$

Table 5.5 Results of Problem 5, stress (ksi),
1 ksi = 6.9 MN/m^2

Node (I,J)	Beam Theory σ_x	Computer Output σ_x	Error %	Node (I,J)	Beam Theory σ_x	Computer Output σ_x	Error %
(11,1)	1.6917			(15,1)	2.3684		
(11,-2)	1.6609	1.726	3.9%	(15,-2)	2.3253	2.419	4.0%
(11,2)	1.6301	1.720	5.5%	(15,2)	2.2822	2.45	7.3%
(11,-3)	1.4665	1.54	5.0%	(15,-3)	2.0531	2.16	5.2%
(11,3)	1.3028	1.35	3.6%	(15,3)	1.8239	1.89	3.6%
(11,-4)	1.1570	1.18	1.9%	(15,-4)	1.6198	1.65	1.8%
(11,4)	1.0111	1.02	0.8%	(15,4)	1.4156	1.42	0.3%
(11,-5)	0.8653	0.852	1.5%	(15,-5)	1.2114	1.19	1.7%
(11,5)	0.7195	0.689	4.2%	(15,5)	1.0073	0.961	4.6%
(11,-6)	0.5736	0.532	7.2%	(15,-6)	0.8031	0.732	8.8%
(11,6)	0.4280	0.376	12.1%	(15,6)	0.5989	0.506	15.5%
(11,-7)	0.2820	0.223	20.9%	(15,-7)	0.3947	0.279	29.3%
(11,7)	0.1361	0.0709	47.9%	(15,7)	0.1906	0.0472	75.2%
(11,-8)	-0.0275	-0.0911	231.3%	(15,-8)	-0.0386	-0.188	387.0%
(11,8)	-0.1912	-0.250	30.7%	(15,8)	-0.2677	-0.411	53.5%
(11,-9)	-0.2220	-0.252	13.5%	(15,-9)	-0.3108	-0.221	28.9%
(11,9)	-0.0297*	-0.0294	1.0%	(15,9)	-0.0416*	-0.0307	26.2%
(11,-10)	-0.0557*	-0.0550	0.1%	(15,-10)	-0.0772*	-0.0783	1.4%
(11,10)	-0.0805*	-0.0805	0%	(15,10)	-0.1127*	-0.1268	12.5%

*Concrete stress

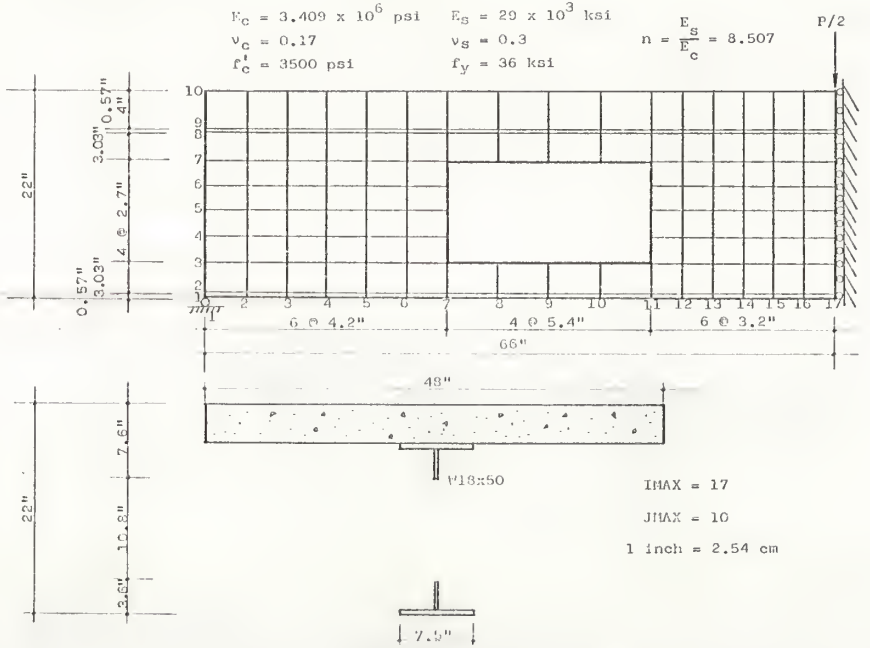

Fig. 5.9 Discretization of Problem 6

Table 5.6 Results of Problem 6, stress (ksi),
1 ksi = 6.9 MN/m^2

Node (I,J)	Vierendeel Method σ_x	Computer Output σ_x	Node (I,J)	Vierendeel Method σ_x	Computer Output σ_x	Node (I,J)	Vierendeel Method σ_x	Computer Output σ_x
(7,1)			(9,1)	1.658		(11,1)	- 2.520	
(7,-2)	3.762	1.154	(9,-2)	1.628	1.753	(11,-2)	- 0.507	-2.377
(7,2)	1.689	1.03	(9,2)	1.598	1.75	(11,2)	1.506	2.6
(7,-3)	- 9.344	3.21	(9,-3)	1.437	1.76	(11,-3)	12.205	-0.015
(7,3)	-20.351	4.99	(9,3)	1.277	1.77	(11,3)	22.905	-2.76
(7,-4)		0.905	(9,-4)			(11,-4)		-0.441
(7,4)		-0.114	(9,4)			(11,4)		0.105
(7,-5)		-0.188	(9,-5)			(11,-5)		0.095
(7,5)		0.036	(9,5)			(11,5)		-0.149
(7,-6)		0.29	(9,-6)			(11,-6)		-0.334
(7,6)		0.16	(9,6)			(11,6)		-0.242
(7,-7)		-1.07	(9,-7)			(11,-7)		-0.936
(7,7)	- 2.057	-4.38	(9,7)	0.133	0.21	(11,7)	2.323	5.01
(7,-8)	- 1.529	-2.84	(9,-8)	-0.027	0.031	(11,-8)	1.475	2.93
(7,8)	- 1.002	-1.65	(9,8)	-0.1874	-0.152	(11,8)	0.627	1.34
(7,-9)	- 0.903	-0.995	(9,-9)	-0.2176	-0.154	(11,-9)	0.467	0.643
(7,9)	- 0.803*	-0.017*	(9,9)	-0.029*	-0.018*	(11,9)	0.036*	0.012*
(7,-10)	- 0.107*	-0.0002*	(9,-10)	-0.054*	-0.046*	(11,-10)	- 0.095*	-0.011*
(7,10)	- 0.589*	-0.017*	(9,10)	-0.079*	-0.073*	(11,10)	- 0.227*	-0.033*

*Concrete Stress

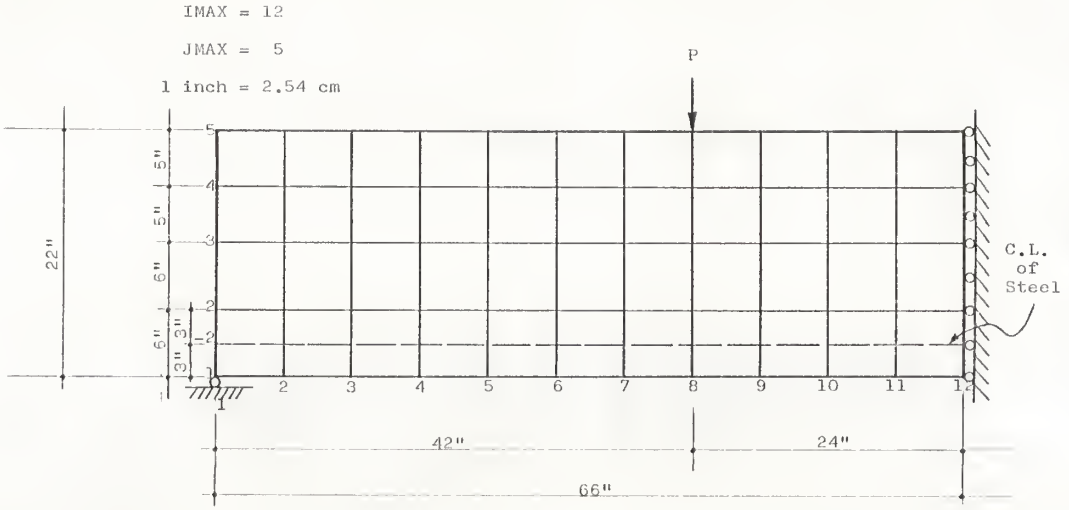

Fig. 5.10 Discretization of Problem 7

where ε_o is the strain corresponding to f'_c. The stress-strain curve was replaced by six linear segments (zones) and the input data is shown in Fig. 5.11 and Appendix B.

A biaxial failure stress plot was assumed to be given by following Kupfer, Holsdorf and Rüsch (15), there are eight sets of data to be given into the program. Fig. 5.12 shows the biaxial failure space and the data is given in Appendix B.

Fig. 5.13 shows the steel properties of the reinforcing bars, f_y = 60 ksi. The normal and tangential bond properties K_n and K_s were assumed to be the Young's modulus of concrete E_c and shear modulus G_c,

$$G_c = \frac{E_c}{2\,(1 + \nu_c)}$$

where E_c, = ν_c are taken as the initial slope of the stress-strain curve (E_I, ν_I).

The resulting crack pattern as predicted by the program at the ends of increments 2 and 3 are shown in Fig. 5.14. Normal stresses were compared with beam theory and are shown in Table 5.7.

5.5.2 Discussion of Results

For the load increment 1, P = 9^k, all sections of the reinforced concrete beam uncracked and the computer results have fairly good agreement with elastic beam theory (See Table 5.7(a)).

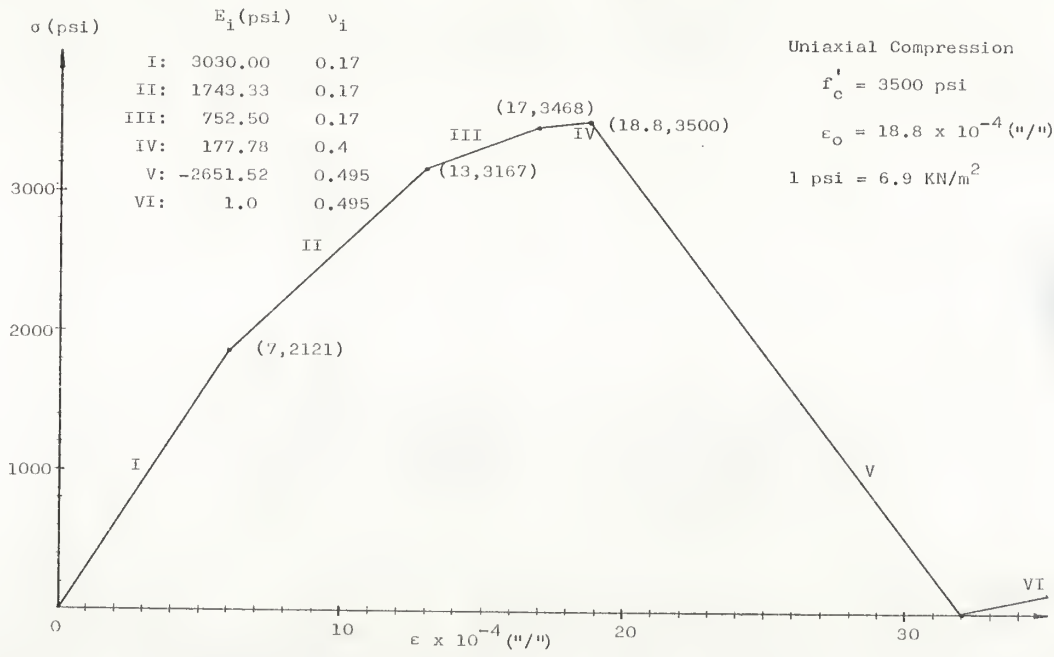

Fig. 5.11 Linearized Stress-Strain Curve of Concrete

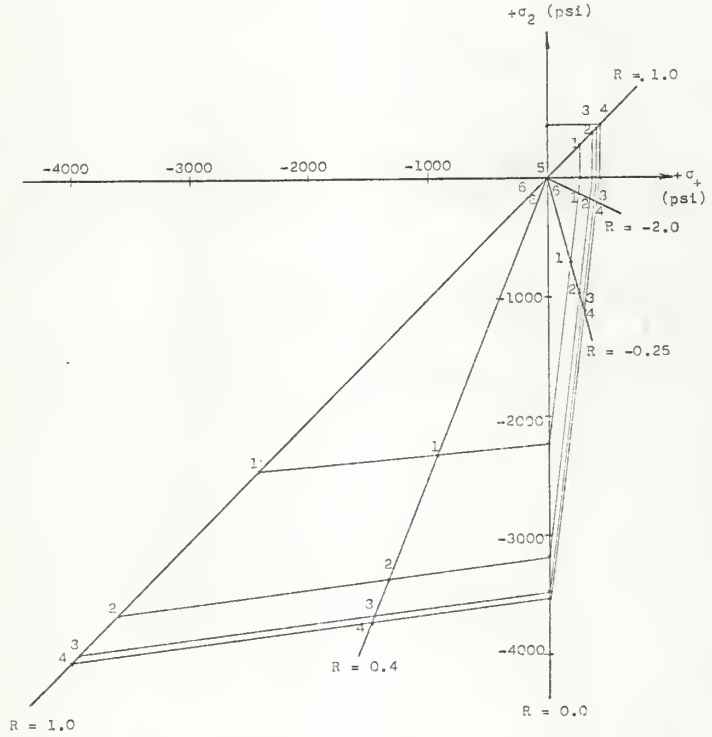

Fig. 5.12 Biaxial Failure Space for Concrete
1 psi = 6.9 KN/m^2

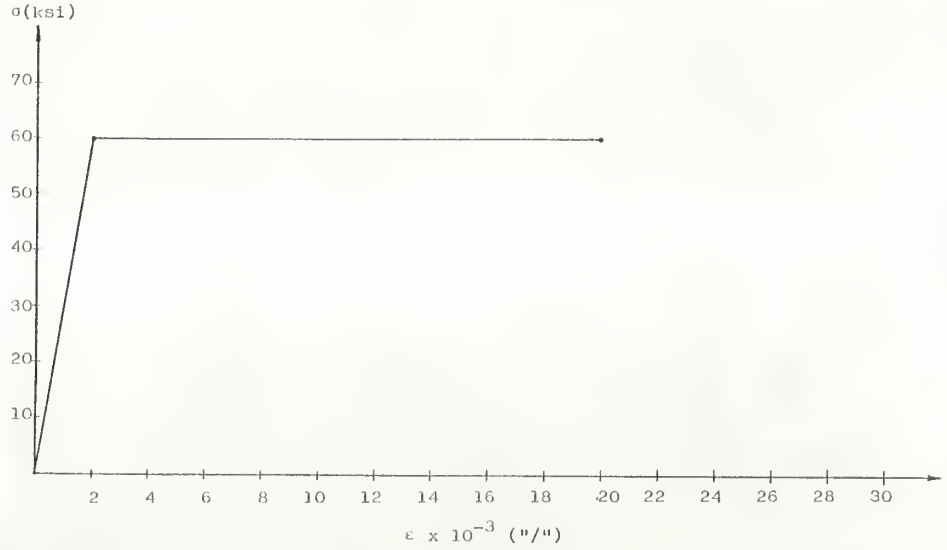

Fig. 5.13 Stress-Strain Curve For Steel
1 psi = 6.9 KN/m^2

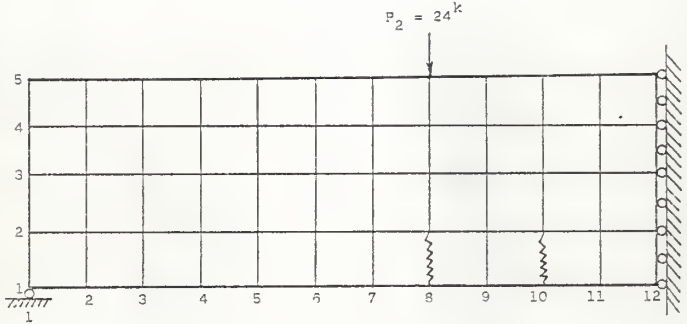

(a) Load Increment 2: $P_2 = 24^k$

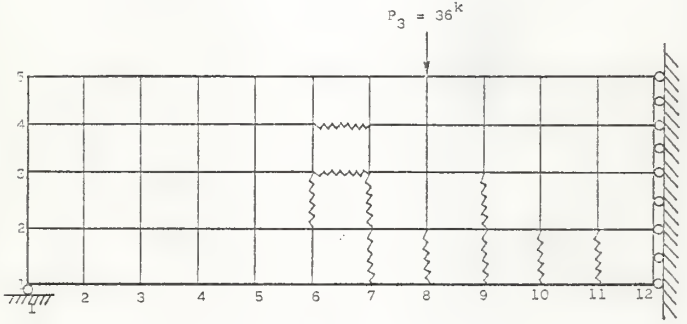

(b) Load Increment 3: $P_3 = 36^k$

Fig. 5.14 Crack Pattern of Problem 7

Table 5.7(a) Stresses (ksi) for Load Increment 1:
$P = 9^k$, 1 ksi = 6.9 MN/m^2
No Cracks

Node (I,J)	Beam Theory σ_x	Computer Output σ_x	Node (I,J)	Beam Theory σ_x	Computer Output σ_x
(4,1)	0.161	0.200	(10,1)	0.377	0.444
(4,-2)	0.114	0.139	(10,-2)	0.266	0.316
Bar	0.981	0.710	Bar	2.289	1.755
(4,2)	0.067	0.078	(10,2)	0.155	0.187
(4,-3)	0.019	0.022	(10-3)	0.045	0.0626
(4,3)	-0.028	-0.030	(10,3)	-0.065	-0.0614
(4,-4)	-0.067	-0.071	(10,-4)	-0.158	-0.165
(4,4)	-0.107	-0.112	(10,4)	-0.250	-0.268
(4,-5)	-0.147	-0.152	(10,-5)	-0.342	-0.365
(4,5)	-0.186	-0.193	(10,5)	-0.434	-0.458

For the load increment 2, P = 24^{k}, uncracked section I = 4 has good agreement with elastic beam theory. The results of cracked section I = 10 are not as good as for uncracked sections. Section I = 6 should crack by beam theory prediction, but the program results are uncracked. Section I = 6 was checked by both cracked and uncracked theory. It can be found out that the computer results at Section I = 6 correspond to cracked beam theory at some locations and uncracked theory at other locations, because the program capability for spacing cracks influences results at adjacent sections (See Table 5.7(b)).

For the load increment 3, P = 36^{k}, uncracked section I = 3 gives fairly reasonable results (See Table 5.7(c)). Other cracked sections were not checked because the stress level in the concrete is greater than about 0.5 f'_c and ordinary beam theory is not adequate for these stress levels.

Table 5.7(b) Stresses (ksi) for Load Increment 2: $P = 24^{k}$, 1 ksi = 6.9 MN/m^2

I = 4 : Uncracked Section

I = 10: Cracked Elastic Behavior Section

I = 6 : Checked by Cracked and Uncracked Beam Theory

Node (I,J)	Beam Theory σ_x	Computer Output σ_x	Node (I,J)	Beam Theory σ_x	Computer Output σ_x	Node (I,J)	Cracked Beam Theory	Uncracked Beam Theory	Computer Output σ_x
(4,1)	0.431	0.500	(10,1)			(6,1)		0.718	.562
(4,-2)	0.304	0.351	(10,-2)			(6,-2)		0.507	.469
Bar	2.587	2.397	Bar	19.354	10.188	Bar	13.825	4.312	5.379
(4,2)	0.178	0.204	(10,2)			(6,2)		0.296	.402
(4,-3)	-0.052	-0.059	(10,-3)			(6,-3)		0.085	.211
(4,3)	-0.075	-0.082	(10,3)			(6,3)		-0.125	- .055
(4,-4)	-0.181	-0.195	(10,-4)	- 0.057	- 0.452	(6,-4)	- 0.0406	-0.301	-0.297
(4,4)	-0.286	-0.306	(10,4)	- 0.564	- 0.847	(6,4)	- 0.403	-0.476	-0.542
(4,-5)	-0.391	-0.410	(10,-5)	- 1.071	- 1.260	(6,-5)	- 0.765	-0.652	-0.771
(4,5)	-0.497	-0.514	(10,5)	- 1.578	- 1.680	(6,5)	- 1.127	-0.828	-0.986

Table 5.7(c) Stresses (ksi) for Load Increment 3:
$P = 36^{k}$, 1 ksi = 6.9 MN/m^2
I = 3: Uncracked Sections

Node (I,J)	Beam Theory σ_x	Computer Output σ_x
(3,1)	0.451	0.606
(3,-2)	0.318	0.388
Bar	2.700	3.334
(3,2)	0.186	0.174
(3,-3)	-0.0537	-0.0151
(3,3)	-0.076	-0.187
(3,-4)	-0.189	-0.245
(3,4)	-0.299	-0.301
(3,-5)	-0.409	-0.348
(3,5)	-0.520	-0.392

CHAPTER VI

CONCLUSIONS

Some modifications were made for the original finite element computer program which was obtained from the University of California at Davis in order to increase the capability of solving bigger matrices and get more accurate numerical solutions.

On the basis of the experiences and numerical results obtained from this study, the following conclusions can be reached:

1. The normal stresses of the non-composite steel beams and composite steel-concrete beams obtained from the finite element computer program had very good agreement with the beam theory (Problems 1, 2, 3, and 5).

2. For the elastic analysis, both steel beams and composite beams (Problems 4 and 6), along the section at the centerline of the opening, the normal stresses obtained from the finite element computer program were close to the predictions based on the Vierendeel Analysis.

3. The normal stresses of uncracked sections and cracked-elastic behavior sections predicted by this program had reasonable agreement with beam theory. However, the program capability exceeds that of normal beam theory in being able to estimate spacing of cracks (Problem 7).

4. The computer program at present cannot predict the ultimate load capacity of a beam system adequately, but it will terminate as an unstable system when the load specified is bigger than the ultimate load capacity.

5. The mesh generation scheme of this program is very awkward to use and effectively prevents the use of a fine mesh at regions of interest in combination with a coarse mesh at other regions. Therefore, very large numbers of elements must be used to adequately model problems such as beams with openings.

6. For the non-linear analysis, for failure the programs need the input of the biaxial stress states or damage of the material. There is great technical difficulty in obtaining these data and they are generally not available.

7. The core storage requirements and running time for a linear analysis are low, but for a non-linear analysis, there are many iterations involved which can raise the running time and cost. A table of core storages, running time and costs for the numerical examples in Chapter V are given in Appendix C.

8. The limits of mesh size capabilities of the program indicated in the documentation vary depending on a number of parameters, eg., number of materials used, "beam" elements used, bond elements used. Further work is necessary to establish appropriate limits on maximum available mesh size that can be used for different combinations of these parameters.

REFERENCES

1. Heller, Brock and Bart, "The Stresses Around a Rectangular Opening With Rounded Corners in a Uniformly Loaded Plate," Proc., 3rd National Congress of Applied Mechanics, 1958.

2. Heller, Brock and Bart, "The Stresses Around a Rectangular Opening With Rounded Corners in a Beam Subjected to Bending and Shear," Proc., 4th National Congress of Applied Mechanics, 1962.

3. Bower, J. E., "Elastic Stresses Around Holes in Wide-Flange Beams," Journal of the Structural Division, American Society of Civil Engineers, Vol. 92, No. ST2, April 1966.

4. Bower, J. E., "Experimental Stresses in Wide Flange Beams With Holes," Journal of the Structural Division, American Society of Civil Engineers, Vol. 92, No. ST5, Proc. Paper 4945, October 1966.

5. Bower, J. E., "Ultimate Strength of Beams With Rectangular Holes," Journal of the Structural Division, ASCE, Vol. 94, No. ST6, June 1968.

6. Redwood, R. G. and McCutcheon, J. O., "Beam Tests With Unreinforced Web Openings," Journal of the Structural Division, ASCE, Vol. 94, No. ST1, Jan. 1968.

7. Cooper, P. B. and Snell, R. R., "Tests on Beams With Reinforced Web Openings," Journal of the Structural Division, ASCE, Vol. 98, No. ST3, March 1972.

8. Viest, I. M., Fountain, R. S. and Singleton, R. C., Composite Construction in Steel and Concrete, McGraw-Hill Book Co., 1958.

9. Viest, I. M., "Review of Research on Composite Steel-Concrete Beams," Journal of the Structural Division, ASCE, Vol. 86, No. ST6, June 1960.

10. Subcommittee on the State-of-the-Art Survey, Task Committee on Composite Construction, "Composite Steel-Concrete Construction," Journal of the Structural Division, ASCE, Vol. 100, No. ST5, May 1974.

11. Giriyappa, J., "Behavior of Composite Castellated Hybrid Beams," M. S. Thesis, Department of Civil Engineering, University of Missouri, Columbia, Mo., May 1966.

12. Larnach, W. J. and Park, R., "The Behavior Under Load of Six Castellated Composite T-Beams," Civil Engineering and Public Works Review, March 1964.

13. Granade, C. J., "An Investigation of Composite Beam Having Large Rectangular Openings in Their Webs," M. S. Thesis, Department of Civil Engineering, University of Alabama, University, Ala., 1968.

14. Taylor, M. A., Romstad, K. M., Herrmann, L. R., and Ramey, M. R., "A Finite Element Computer Program for the Prediction of the Behavior of Reinforced and Prestressed Concrete Structures Subject to Cracking," University of California at Davis, No. N62399-70-C-0023, June 1, 1972.

15. Kupfer, H., Hilsdorf, H., and Rüsch, H., "Behavior of Concrete Under Biaxial Stresses," Journal of American Concrete Institute, Proceedings V. 66, August 1969.

16. Ngo, D. and Scordelis, A., "Finite Element Analysis of Reinforced Concrete Beams," ACI Journal, Proceedings V. 64, No. 3, March 1967, pp. 152-163.

17. Nilson, A., "Nonlinear Analysis of Reinforced Concrete by the Finite Element Method," ACI Journal, Proceedings V. 65, No. 9, September 1968, pp. 757-766.

18. Oktay, Ural, Finite Element Method, New York: Intext Educational Publishers, 1976.

19. Timoshenko, S. P., Theory of Plates and Shells, McGraw-Hill Book Company, 1959.

20. Herrmann, L. R., Final Report to NCEL, August 1, 1970. Ref. Contract N62399-70-M-0015.

21. Wilson, E. L., "Structural Analysis of Axisymmetric Solids," AIAA Paper No. 65-143, Jan. 1965.

APPENDIX A

CHANGING THE DIMENSIONS OF TAYLOR'S PROGRAM

When changing the dimensions of the program, three areas must be considered:

1. Common blocks (See Table A.1)
2. The values of IZT and NQMAX specified at the beginning of the program MAIN
3. The dimension checks at the end of the subroutine PREP.

The dimensions in the program which are related to the size of the problem are indicated below:

CPI (N_1, 3, 4)

F (N_1, 2)

AL (N_1, 5)

TCEXP (N_1), NONPRC (N_1)

ZE (N_1, N_2), ZNU (N_1, N_2)

ES1 (N_2), ES2 (N_2), EMOD (N_2), ENU (N_2)

R (N_1, N_3)

ZEI (N_1, N_3, N_2), ZE2 (N_1, N_3, N_2)

NONPRB (N_4), XIBA (N_4), ABA (N_4), EBA (N_4), EBAP (N_4), ALPBA (N_4)

TBOVER (N_4), SCFBA (N_4), GNUBA (N_4)

ZSB (N_{16}, N_5), ZEB (N_{16}, N_5)

NONPRO (N_6)

XKN (N_6, 4), XKS (N_6, 4)

Z3BN (N_7), ZEBN (N_7), Z3BS (N_7), ZEBS (N_7)

PSTRN (N_1, 4)

PSBM (N_4, 2)

NODB (N_8)

BIV (N_8, 3)

NEA (N_9)

T (N_{10}, N_{11})

X (N_{10}, N_{11}), Y(N_{10}, N_{11}), MNO(N_{10}, N_{11})

S (N_{12})

NQ (N_{15})

NONLA (N_{13})

CRAK (N_{14}, N_{11})

IZT = N_{12}

NOMAX = N_{15}

Where:

N_1 = maximum number of continuum materials (must not exceed 9)

N_2^{-1} = maximum number of zones in a continuum stress strain representation

N_3 = maximum number of stress ratios used in the description of a continuum stress-strain surface

N_4 = maximum number of beam types (must not exceed 9)

N_5 = maximum number of zones in a beam or bond stress-strain representation

N_6 = maximum number of different bond descriptions (must not exceed 9)

N_7 = maximum number of zones in the bond description

N_8^{-1} = maximum number of boundary conditions

N_9^{-1} = $2 N_{10} N_{11} - N_{10} - N_{11}$

N_{10} = maximum value of IMAX

N_{11} = maximum value of JMAX

N_{12} = size of core equation block

N_{13} = (N_{10}^{-1}) (N_{11}^{-1})

N_{14} = $2 N_{10}^{-1}$

N_{15}^{-1} = maximum number of system unknowns (the actual number for a given problem is dependent upon the degree of cracking - it is suggested that $N_{15} = 8 N_{10} N_{11}$)

N_{16} = $N_4 + N_6$

Values of Above Dimensions of the Current Program

N_1 =	3	N_9 =	1000
N_2 =	7	N_{10} =	21
N_3 =	10	N_{11} =	11
N_4 =	4	N_{12} =	28500
N_5 =	8	N_{13} =	231
N_6 =	3	N_{14} =	44
N_7 =	10	N_{15} =	1000
N_8 =	100	N_{16} =	10

SUBROUTINE \ COMMON BLOCK	1	2	3	4	5	6	7	8	9
MAIN	X	X	X	X	X	X	X	X	
SOLPRT		X	X		X	X			
BLOCK DATA			X			X			
FNOD		X				X			
BEST	X	X	X	X					
BONDST									
ELST	X	X	X	X	X	X		X	
PREP	X	X	X	X	X	X		X	
MAXV									
BUNARY		X							
STIFNS	X	X	X		X				
ELIM			X						
RESTRN			X						
ROTAT			X						
STFSUB	X	X	X		X		X		
TINTGR							X		X*
REDUCT				X					X*
BAKSUB				X					
PRINC									
COMPEL	X	X	X						
COMBIN			X						
BONDEL	X		X						
BEAMEL	X	X	X				X		
EVAL							X		
CRAKD						X			
CRKING		X	X			X		X	
CONVRT	X								
PROPEC	X		X						
PROPER	X		X		X			X	
PROPEB	X		X					X	
FAILU	X		X	X					

*Due to double precisioning this subroutine.

Table A.1 Common Blocks - Subroutine Association

```
        PROB. N-I-2-1-1
 ----------------------------------------------------------------------

PLANE STRESS ANALYSIS - THICKNESS STRESS =  0.0
                    THICKNESS=  1.00E 01

                        I-MAX =  12

                        J-MAX =  5

                NUMBER OF INCREMENTS=  3


PRIO LINE SPACING BETWEEN INITIAL CRACKS=  1



            MAX NUMBER OF ITERATIONS=  16

                MAX AVERAGE ERROR=    0.0200


PROPERTIES FOR MATERIAL  1
                 ************************

          F-X OR F-R        F-Y OR F-Z          E              NU          ALPHA
          0.0               0.0             3.03E 03       1.70E-01      0.0


     NONLINEAR PROPERTIES FOR CONTINUUM MATERIAL  1

  NUMBER OF ZONES  6          NUMBER OF RADIAL STRESS LINES  8

ZONE NUMBER   MODULUS      POISSON

     1       3.0300E 03  1.7000E-01
     2       1.7433E 03  1.7000E-01
     3       7.5250E 02  1.7000E-01
     4       1.7778E 02  4.0000E-01
     5      -2.6515E 03  4.5500E-01
     6       1.0000E 00  4.5500E-01
```

TRESS RATIO	PRINCIPAL STRESS LEVELS****STARTING FROM COMP-COMP****					
1.0000	-0.2439E 01	-0.3624E 01	-0.3588E 01	-0.4025E 01	0.0	-0.5000E-01
0.4000	-0.2310E 01	-0.3350E 01	-0.3650E 01	-0.3700E 01	0.0	-0.5000E-01
0.0	-0.2121E 01	-0.3167E 01	-0.3468E 01	-0.3500E 01	0.0	-0.5000E-01
-0.2500	-0.1720E 00	-0.1030E 01	-0.1120E 01	-0.1180E 01	0.0	-0.5000E-01
-2.0000	-0.1400E 00	-0.1800E 00	-0.2000E 00	-0.2200E 00	0.0	-0.5000E-01
-20.0000	-0.1400E-01	-0.1500E-01	-0.2100E-01	-0.2220E-01	0.0	-0.5000E-03
20.0000	0.2800E 00	0.3800E 00	0.4200E 00	0.4440E 00	0.0	0.5000E-01
1.0000	0.2800E 00	0.3800E 00	0.4200E 00	0.4440E 00	0.0	0.5000E-01

****

BEAM PROPERTIES
****

MOM. INERT.	AREA	YOUNGS MOD	ALPHA	OVERLAY THICKNESS	S.C.F.	POISSONS RATIO
1.563E-01	3.140E 00	2.900E 04	0.0	9.000E 00	1.128E 00	3.000E-01

NONLINEAR PROPERTIES FOR BEAM MATERIAL 1

NUMBER OF POINTS 2

BREAK POINT	STRESS	STRAIN
1	6.0000E 01	2.0690E-03
2	6.0000E 01	2.0000E-02

****

BEAM PROPERTIES

INITIAL BEAD MODULUS**NORMAL***TANGENTIAL
3030. 1295.

*****BOUNDARY CONDITIONS*****

BOUNDARY POINT DESCRIPTION

1	1	1	PX=	0.0	UY=	0.0	TH=	0.0	PRES=	0.0
2	12	1	UX=	0.0	PY=	0.0	TH=	0.0	PRES=	0.0
3	12	-2	UX=	0.0	PY=	0.0	TH=	0.0	PRES=	0.0
4	12	2	UX=	0.0	PY=	0.0	TH=	0.0	PRES=	0.0
5	12	-3	UX=	0.0	PY=	0.0	TH=	0.0	PRES=	0.0
6	12	3	UX=	0.0	PY=	0.0	TH=	0.0	PRES=	0.0
7	12	-4	UX=	0.0	PY=	0.0	TH=	0.0	PRES=	0.0
8	12	4	UX=	0.0	PY=	0.0	TH=	0.0	PRES=	0.0
9	12	-5	UX=	0.0	PY=	0.0	TH=	0.0	PRES=	0.0
10	12	5	UX=	0.0	PY=	0.0	TH=	0.0	PRES=	0.0
11	8	5	PX=	0.0	PY=	-1.00E 00	TH=	0.0	PRES=	0.0

GEOMETRIC DESCRIPTION OF BEAM ELEMENT

IM - JB	MB	IE - JE	ME	MAT-NO	BOND
1 -2	0	12 -2	1	1	1

****

INCREMENTAL PROPORTION OF TOTAL LOAD OR DISPL. BODY FORCE AND TEMPERATURE

LOAD-DISPL= 0.90DE 01 FORCE= 0.0 TEMP= 0.0

*****GEOMETRY*****

NODE	POINT	X-Y COORDINATES		TEMP. CHANGE
1	1	0.0	0.0	0.0
1	-2	0.0	3.00E 00	0.0
1	2	0.0	6.00E 00	0.0
1	3	0.0	1.20E 01	0.0
1	4	0.0	1.70E 01	0.0
1	5	0.0	2.20E 01	0.0
2	1	6.00E 00	0.0	0.0
2	-2	6.00E 00	3.00E 00	0.0
2	2	6.00E 00	6.00E 00	0.0
2	3	6.00E 00	1.20E 01	0.0
2	4	6.00E 00	1.70E 01	0.0
2	5	6.00E 00	2.20E 01	0.0
3	1	1.20E 01	0.0	0.0
3	-2	1.20E 01	3.00E 00	0.0
3	2	1.20E 01	6.00E 00	0.0
3	3	1.20E 01	1.20E 01	0.0
3	4	1.20E 01	1.70E 01	0.0
3	5	1.20E 01	2.20E 01	0.0
4	1	1.80E 01	0.0	0.0
4	-2	1.80E 01	3.00E 00	0.0
4	2	1.80E 01	6.00E 00	0.0
4	3	1.80E 01	1.20E 01	0.0
4	4	1.80E 01	1.70E 01	0.0
4	5	1.80E 01	2.20E 01	0.0
5	1	2.40E 01	0.0	0.0
5	-2	2.40E 01	3.00E 00	0.0
5	2	2.40E 01	6.00E 00	0.0
5	3	2.40E 01	1.20E 01	0.0
5	4	2.40E 01	1.70E 01	0.0
5	5	2.40E 01	2.20E 01	0.0
6	1	3.00E 01	0.0	0.0
6	-2	3.00E 01	3.00E 00	0.0
6	2	3.00E 01	6.00E 00	0.0
6	3	3.00E 01	1.20E 01	0.0
6	4	3.00E 01	1.70E 01	0.0
6	5	3.00E 01	2.20E 01	0.0
7	1	3.60E 01	0.0	0.0
7	-2	3.60E 01	3.00E 00	0.0
7	2	3.60E 01	6.00E 00	0.0
7	3	3.60E 01	1.20E 01	0.0
7	4	3.60E 01	1.70E 01	0.0
7	5	3.60E 01	2.20E 01	0.0
8	1	4.20E 01	0.0	0.0
8	-2	4.20E 01	3.00E 00	0.0
8	2	4.20E 01	6.00E 00	0.0
8	3	4.20E 01	1.20E 01	0.0
8	4	4.20E 01	1.70E 01	0.0
8	5	4.20E 01	2.20E 01	0.0
9	1	4.80E 01	0.0	0.0
9	-2	4.80E 01	3.00E 00	0.0
9	2	4.80E 01	6.00E 00	0.0
9	3	4.80E 01	1.20E 01	0.0
9	4	4.80E 01	1.70E 01	0.0
9	5	4.80E 01	2.20E 01	0.0
10	1	5.40E 01	0.0	0.0

10	-2	5.40E 01	3.00E 00	0.0
10	2	5.40E 01	6.00E 00	0.0
10	3	5.40E 01	1.20E 01	0.0
10	4	5.40E 01	1.70E 01	0.0
10	5	5.40E 01	2.20E 01	0.0
11	1	6.00E 01	0.0	0.0
11	-2	6.00E 01	3.00E 00	0.0
11	2	6.00E 01	6.00E 00	0.0
11	3	6.00E 01	1.20E 01	0.0
11	4	6.00E 01	1.70E 01	0.0
11	5	6.00E 01	2.20E 01	0.0
12	1	6.60E 01	0.0	0.0
12	-2	6.60E 01	3.00E 00	0.0
12	2	6.60E 01	6.00E 00	0.0
12	3	6.60E 01	1.20E 01	0.0
12	4	6.60E 01	1.70E 01	0.0
12	5	6.60E 01	2.20E 01	0.0

```
NCREMENTAL PROPORTION OF TOTAL LOAD OR DISPL. BODY FORCE AND TEMPERATURE

LOAD-DISPL=       0.120E 02   FORCE=       0.0          TEMP=       0.0

U-V DISPLACEMENTS FOR NODE     8     1 PREDICTED IN ITERATION  0
2   -0.185E-01   -0.701E-01
4   -0.110E-01   -0.686E-01

     CRACK DEVELOPED ALONG LINE  11   1  --  11   2   IN ITERATION   0

     CRACK DEVELOPED ALONG LINE   7   1  --   7   2   IN ITERATION   0

     CRACK DEVELOPED ALONG LINE   7   2  --   7   3   IN ITERATION   0

     CRACK DEVELOPED ALONG LINE   9   2  --   9   3   IN ITERATION   0


U-V DISPLACEMENTS FOR NODE     8     1 PREDICTED IN ITERATION  1
2   -0.555E-02   -0.835E-01
4   -0.103E-01   -0.863E-01

     CRACK DEVELOPED ALONG LINE   6   3  --   7   3   IN ITERATION   1

     CRACK DEVELOPED ALONG LINE   9   1  --   9   2   IN ITERATION   1

     CRACK DEVELOPED ALONG LINE   6   2  --   6   3   IN ITERATION   1


U-V DISPLACEMENTS FOR NODE     8     1 PREDICTED IN ITERATION  2
2   -0.155E-01   -0.953E-01
4   -0.954E-01   -0.986E-01


ITERATION CONVERGENCE INFORMATION    2


          AVERAGE SECANT MODULUS ERROR=    0.0693


U-V DISPLACEMENTS FOR NODE     8     1 PREDICTED IN ITERATION  3
2   -0.161E-01   -0.102E 00
4   -0.233E-01   -0.102E 00

     CRACK DEVELOPED ALONG LINE   6   4  --   7   4   IN ITERATION   3


U-V DISPLACEMENTS FOR NODE     8     1 PREDICTED IN ITERATION  4
```

```
2   -C.157E-01   -C.104E 00
4   -0.227E-01   -0.104E 00

.

TERATION CONVERGENCE INFORMATION    4

        AVERAGE SECANT MODULUS ERROR=    0.0144
```

SOLUTION FOR INCREMENT 3 REQUIRED 4 ITERATIONS

****

STRESSES AND STRAINS

PO	NODE	U	V	E-X	E-Y	GAM-XY	E-Z	S-X	S-Y	S-XY	S-Z	S-1	S-2	TH
4	1 1	-6.80E-02	0.0	1.70E-04	-5.01E-04	-8.54E-04	6.76E-05	2.40E-01	-1.32E 00	-9.94E-01	0.0	7.23E-01	-1.80E 00	-2.59E 01
2	1 -2	-3.54E-02	-4.68E-03	2.02E-04	-7.86E-04	-2.35E-04	1.20E-04	1.93E-01	-2.10E 00	-2.80E-01	0.0	2.26E-01	-2.14E 00	-6.84E 00
	L= -3.542E-02	V= -4.684E-03	P= -1.368E-01	M= 4.039E-02	V= -1.618E-02	PZ (ORPHI 0.0								
	SR#1= 0.0	SAS1= 0.0	SR#2= -2.450E-02	SAS2= -5.265E-01										
3	1 2	-3.58E-02	-4.71E-03	1.90E-05	-5.81E-04	2.66E-05	1.15E-04	-2.30E-01	-1.68E 00	1.35E-02	0.0	-2.30E-01	-1.68E 00	5.36E-01
2	1 -3	-2.15E-02	-5.66E-03	2.94E-05	-2.59E-04	-1.35E-04	4.69E-05	-4.53E-02	-7.91E-01	-1.74E-01	0.0	-6.61E-03	-8.30E-01	-1.25E 01
3	1 3	-7.37E-03	-6.26E-03	3.15E-05	-1.36E-04	-4.14E-05	2.14E-05	2.62E-02	-4.07E-01	-5.36E-02	0.0	3.27E-02	-4.14E-01	-6.96E 00
2	1 -4	4.47E-03	-6.45E-03	1.19E-05	-5.44E-05	-2.21E-05	8.70E-06	8.41E-03	-1.63E-01	-2.86E-02	0.0	1.30E-02	-1.68E-01	-9.20E 00
3	1 4	1.64E-02	-6.54E-03	2.08E-06	-1.10E-05	-2.24E-06	1.84E-06	6.23E-04	-3.34E-02	-2.90E-03	0.0	8.68E-04	-3.36E-02	-4.84E 00
2	1 -5	2.83E-02	-6.55E-03	3.78E-06	2.51E-07	1.45E-05	-8.26E-07	1.19E-02	2.79E-03	1.88E-02	0.0	2.67E-02	-1.20E-02	3.82E 01
3	1 5	4.04E-02	-6.54E-03	1.08E-05	4.53E-06	3.28E-05	-3.13E-06	3.60E-02	1.99E-02	4.24E-02	0.0	7.11E-02	-1.52E-02	3.56E 01
2	-2 1	-6.77E-02	-1.48E-02	2.35E-04	-1.18E-04	-4.08E-04	-2.40E-05	6.05E-01	-2.18E-01	-4.73E-01	0.0	8.20E-01	-4.33E-01	-2.45E 01
1	-2 2	-3.58E-02	-1.49E-02	-3.03E-05	-2.21E-04	-8.71E-05	5.15E-05	-2.00E-01	-6.66E-01	-1.20E-01	0.0	-1.71E-01	-6.95E-01	-1.36E 01
1	-2 3	-7.32E-03	-2.07E-02	6.12E-07	-9.70E-05	-1.60E-04	1.97E-05	-4.95E-02	-3.02E-01	-2.08E-01	0.0	6.71E-02	-4.19E-01	-2.93E 01
1	-2 4	1.64E-02	-2.10E-02	-1.23E-05	-1.56E-05	-6.95E-05	6.53E-06	-4.88E-02	-6.77E-02	-8.99E-02	0.0	3.22E-02	-1.49E-01	-4.20E 01
1	-2 5	4.04E-02	-2.10E-02	-6.42E-07	7.61E-07	1.32E-05	-2.43E-08	-1.60E-03	2.03E-03	1.72E-02	0.0	1.75E-02	-1.70E-02	4.80E 01
2	2 1	-6.66E-02	-3.51E-02	3.60E-04	-2.04E-05	5.92E-05	-6.95E-05	1.03E 00	1.17E-01	6.81E-02	0.0	1.04E 00	1.12E-01	4.23E 00
1	2 -2	-3.53E-02	-3.52E-02	1.37E-04	-2.04E-05	1.05E-04	-2.39E-05	3.93E-01	7.87E-03	1.21E-01	0.0	4.28E-01	-2.71E-02	1.61E 01
	L= -3.531E-02	V= -3.517E-02	P= 3.511E 00	M= -9.190E-02	V= -1.072E-02	PZ (ORPHI 0.0								

```
     SBN1=  0.0        SBS1=  0.0        SBN2= -1.748E-02  SBS2= -9.062E-01

   2    2
1 -3.60E-02 -3.52E-02 -5.79E-05  1.94E-05 -9.97E-05  7.89E-06 -1.62E-01  2.02E-02 -1.33E-01  0.0       9.03E-02 -2.32E-01 1.18E 02

   2   -3
1 -2.16E-02 -3.53E-02 -3.35E-05 -3.57E-05 -2.55E-04  1.50E-05 -1.25E-01 -1.41E-01 -3.24E-01  0.0       1.91E-01 -4.57E-01-4.43E 01

   2    3
1 -7.37E-03 -3.54E-02 -3.24E-05 -4.17E-05 -2.62E-04  1.52E-05 -1.23E-01 -1.47E-01 -3.39E-01  0.0       2.04E-01 -4.75E-01-4.49E 01

   2   -4
1  4.44E-03 -3.55E-02 -3.56E-05 -2.79E-05 -2.08E-04  1.31E-05 -1.27E-01 -1.06E-01 -2.66E-01  0.0       1.50E-01 -3.83E-01 1.34E 02

   2    4
1  1.63E-02 -3.56E-02 -3.64E-05 -1.40E-05 -1.42E-04  1.03E-05 -1.21E-01 -6.30E-02 -1.84E-01  0.0       9.46E-02 -2.79E-01 1.31E 02

   2   -5
1  2.83E-02 -3.56E-02 -3.11E-05 -2.92E-06 -7.26E-05  6.96E-06 -9.85E-02 -2.56E-02 -9.33E-02  0.0       3.81E-02 -1.62E-01 1.24E 02

   2    5
1  4.04E-02 -3.56E-02 -2.17E-05  3.25E-06 -8.73E-06  3.78E-06 -6.60E-02 -1.36E-03 -1.13E-02  0.0       5.62E-04 -6.79E-02 9.96E 01

  -3    1
2 -6.59E-02 -5.02E-02  2.09E-04 -2.60E-05 -8.14E-07 -3.75E-05  6.38E-01  2.98E-02 -1.05E-03  0.0       6.38E-01  2.98E-02-9.93E-02

  -3    2
1 -3.60E-02 -5.03E-02  1.22E-05 -5.80E-06 -1.02E-04 -1.31E-06  3.49E-02 -1.16E-02 -1.32E-01  0.0       1.46E-01 -1.23E-01-4.00E 01

  -3    3
1 -7.49E-03 -5.03E-02 -4.83E-05 -6.00E-06 -2.46E-04  1.11E-05 -1.54E-01 -4.43E-02 -3.21E-01  0.0       2.26E-01 -4.25E-01 1.30E 02

  -3    4
1  1.61E-02 -5.03E-02 -6.93E-05  5.43E-06 -1.66E-04  1.31E-05 -2.13E-01 -1.98E-02 -2.07E-01  0.0       1.12E-01 -3.45E-01 1.22E 02

  -3    5
1  4.02E-02 -5.02E-02 -7.41E-05  1.57E-05 -1.24E-05  1.20E-05 -2.23E-01  9.68E-03 -1.60E-02  0.0       1.08E-02 -2.24E-01 9.39E 01

   3    1
2 -6.59E-02 -6.50E-02  2.00E-04 -2.22E-05 -3.91E-06 -3.64E-05  6.06E-01  3.64E-02 -5.40E-03  0.0       6.06E-01  3.63E-02-5.43E-01

   3   -2
1 -3.48E-02 -6.51E-02  1.28E-04 -1.79E-05 -1.03E-05 -2.27E-05  3.88E-01  1.24E-02 -1.38E-02  0.0       3.88E-01  1.19E-02-2.10E 00
  L= -3.444E-02  Y= -6.514E-02  P=  1.047E 01  M= -1.358E-01  V= -3.693E-03  PZ EORPM1  0.0
     SBN1=  0.0        SBS1=  0.0        SBN2=  3.142E-03  SBS2= -1.409E 00

   3    2
1 -3.59E-02 -6.51E-02  5.84E-05 -1.07E-05 -9.14E-05 -9.77E-06  1.74E-01 -2.34E-03 -1.16E-01  0.0       2.31E-01 -5.96E-02-2.64E 01

   3   -3
1 -2.17E-02 -6.51E-02 -6.73E-06  7.85E-06 -2.06E-04 -2.31E-07 -1.51E-02  2.09E-02 -2.60E-01  0.0       2.64E-01 -2.58E-01 1.33E 02

   3    3
1 -7.66E-03 -6.51E-02 -6.47E-05  2.17E-05 -2.43E-04  8.80E-06 -1.87E-01  3.30E-02 -3.11E-01  0.0       2.52E-01 -4.07E-01 1.25E 02

   3   -4
1  4.68E-03 -6.51E-02 -8.11E-05  1.56E-05 -2.11E-04  1.34E-05 -2.45E-01  5.64E-03 -2.73E-01  0.0       1.81E-01 -4.20E-01 1.23E 02
```

```
   3    4
1  1.59E-02 -6.50E-02 -9.95E-05  1.77E-05 -1.74E-04  1.68E-05 -3.01E-01  2.36E-03 -2.26E-01  0.0      1.23E-01 -4.21E-01 1.18E 02
                                        2
   3   -5
1  2.78E-02 -6.50E-02 -1.15E-04  2.04E-05 -9.42E-05  1.94E-05 -3.48E-01  2.61E-03 -1.22E-01  0.0      4.08E-02 -3.87E-01 1.07E 02

   3    5
1  3.59E-02 -6.49E-02 -1.30E-04  2.45E-05 -1.26E-05  2.16E-05 -3.92E-01  7.48E-03 -1.64E-02  0.0      8.15E-03 -3.93E-01 9.23E 01

  -4    1
2 -6.47E-02 -7.96E-02  1.95E-04 -2.58E-05 -1.55E-07 -3.37E-05  5.82E-01  1.10E-02 -2.01E-03  0.0      5.82E-01  1.10E-02-2.02E-01

  -4    2
1 -3.57E-02 -7.98E-02  8.03E-05 -1.99E-05 -1.02E-04 -1.24E-05  2.33E-01 -1.74E-02 -1.25E-01  0.0      2.85E-01 -6.95E-02-2.25E 01

  -4    3
1 -7.84E-03 -7.98E-02 -6.26E-05  1.76E-05 -2.46E-04  9.21E-06 -1.80E-01  2.12E-02 -3.10E-01  0.0      2.46E-01 -4.05E-01 1.26E 02

  -4    4
1  1.55E-02 -7.97E-02 -1.31E-04  2.60E-05 -1.63E-04  2.14E-05 -3.94E-01  1.19E-02 -2.11E-01  0.0      1.02E-01 -4.84E-01 1.13E 02

  -4    5
1  3.54E-02 -7.95E-02 -1.81E-04  3.10E-05 -4.86E-06  3.08E-05 -5.49E-01 -4.87E-05 -6.29E-03  0.0      2.33E-05 -5.49E-01 9.07E 01

   4    1
2 -6.41E-02 -9.40E-02  2.02E-04 -3.83E-05  8.32E-06 -3.35E-05  5.80E-01 -6.25E-03  3.37E-03  0.0      5.80E-01 -6.27E-03 3.30E-01

   4   -2
1 -3.38E-02 -9.43E-02  1.62E-04 -3.83E-05  6.76E-06 -2.52E-05  4.49E-01 -2.85E-02 -7.79E-04  0.0      4.49E-01 -2.85E-02-9.35E-02
  L= -3.382F-02  Y= -5.427E-02  P=  2.657E 01  H= -1.353E-01  V= -5.103E-03  PI (ORPH)  0.0
     SHM1=  0.0        SBS1=  0.0        SBN2= -6.472E-04  SBS2= -2.112E 00


   4    2
1 -3.54E-02 -9.43E-02  1.15E-04 -4.60E-05 -1.12E-04 -1.53E-05  3.10E-01 -5.29E-02 -1.38E-01  0.0      3.57E-01 -9.92E-02-1.86E 01

   4   -1
1 -2.17E-02 -9.43E-02  2.18E-05 -1.22E-05 -2.44E-04 -1.97E-06  6.08E-02 -2.23E-02 -2.95E-01  0.0      3.17E-01 -2.79E-01-4.10E 01

   4    3
1 -8.03E-03 -9.43E-02 -6.56E-05  1.06E-05 -2.60E-04  1.13E-05 -1.91E-01 -1.25E-03 -3.25E-01  0.0      2.42E-01 -4.35E-01 1.27E 02

   4   -4
1  3.47E-03 -9.43E-02 -1.17E-04  2.19E-05 -2.06E-04  1.94E-05 -3.52E-01  6.65E-03 -2.66E-01  0.0      1.49E-01 -4.94E-01 1.18E 02

   4    4
1  1.51E-02 -9.42E-02 -1.65E-04  3.47E-05 -1.56E-04  2.67E-05 -4.97E-01  2.07E-02 -2.02E-01  0.0      9.05E-02 -5.67E-01 1.09E 02

   4   -5
1  2.69E-02 -9.42E-02 -1.98E-04  3.49E-05 -8.10E-05  3.33E-05 -5.58E-01  4.25E-03 -1.05E-01  0.0      2.20E-02 -6.16E-01 9.96E 01

   4    5
1  3.88E-02 -9.41E-02 -2.28E-04  3.88E-05 -1.80E-06  3.88E-05 -6.91E-01  1.16E-04 -2.34E-03  0.0      1.24E-04 -6.91E-01 9.02E 01

  -5    1
2 -6.36E-02 -1.08E-01  1.62E-04 -3.51E-05  4.73E-05 -2.63E-05  4.84E-01 -1.10E-02  3.88E-02  0.0      4.87E-01 -1.40E-02 4.46E 00

  -5    2
1 -3.50E-02 -1.09E-01  1.56E-04 -5.56E-05 -5.24E-05 -1.97E-05  4.03E-01 -8.48E-02 -1.21E-01  0.0      4.32E-01 -1.13E-01-1.32E 01
```

APPENDIX C

CORE STORAGE REQUIREMENTS, RUNNING TIME AND COSTS FOR NUMERICAL EXAMPLES

IBM 370/158 computer system was used for solving all the numerical examples presented in Chapter V. Table C.1 shows the core used, running time and costs of these examples.

Table C.1

Problem	(IMAX, JMAX)	Core Used (k)	Running Time (seconds)	Cost (Dollars)
1	(21,8)	266k*	43.98	15.33
2	(21,7)	266k*	39.77	13.89
3	(21,9)	266k*	58.72	20.17
4	(21,9)	266k*	43.54	15.22
5	(17,10)	266k*	59.22	20.27
6	(17,10)	484k**	49.35	23.73
7	(12,5)	480k**	133.86	62.56

*Small version of the program: IZT = 6000

**Large version of the program: IZT = 28500 (See Appendix A)

ACKNOWLEDGMENTS

The author wishes to express his sincere appreciation to his major professor, Dr. Stuart E. Swartz, without whose assistance and continuing encouragement and guidance this thesis would not have been possible.

Appreciation is extended to my committee members, Dr. Peter B. Cooper and Dr. Hugh S. Walker for their instruction in those courses which were related to the writing of this thesis.

Gratitude is due to the author's parents whose encouragement contributed much toward the successful completion of this thesis.

I would also like to extend my sincere thanks to Dr. Robert R. Snell, Head of the Civil Engineering Department, and to the National Science Foundation for their financial support through Grant No. ENG76-19045.

EVALUATION OF A FINITE-ELEMENT METHOD TO ANALYZE STEEL AND CONCRETE STRUCTURAL MEMBERS

by

DAVID DAHWEI LEE

B.S., Taiwan Provincial College of Marine and Oceanic Technology, 1974

AN ABSTRACT OF A MASTER'S THESIS

submitted in partial fulfillment of the

requirements for the degree

MASTER OF SCIENCE

Department of Civil Engineering

KANSAS STATE UNIVERSITY
Manhattan, Kansas

1978

ABSTRACT

A finite element computer program which was developed in the University of California at Davis was used to model non-composite steel beams, reinforced concrete beams, composite steel concrete beams without web openings and composite steel-concrete beams with web openings. The numerical results obtained from the finite element computer program analysis had generally good agreement with those obtained from other methods of analysis.

Although research investigations of the behavior of non-composite steel beams with web openings and the elastic behavior of composite steel-concrete beams have been conducted in past years, the results of these investigations cannot be directly applied to composite steel-concrete beams with web openings.

On the basis of experiences and the results of numerical examples, some conclusions of the suitability and limitations of this program were reached in this study.

It was generally concluded that this computer program has the capability of adequately modelling the composite beam with web opening. However, the cost/storage requirements for this program may preclude its extensive application to this problem.